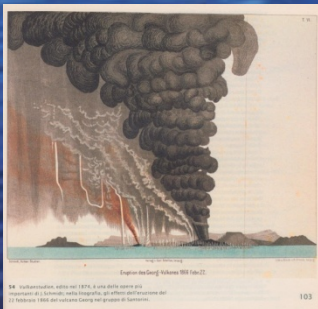




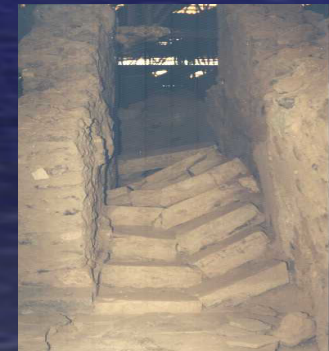
Fault geometry and kinematics of the broader Santorini area in relation to seismic activity and volcanism

Spyros B. Pavlides

*Department of Geology, Aristotle University of Thessaloniki,
54124 Thessaloniki, Greece
Pavlides@geo.auth.gr*



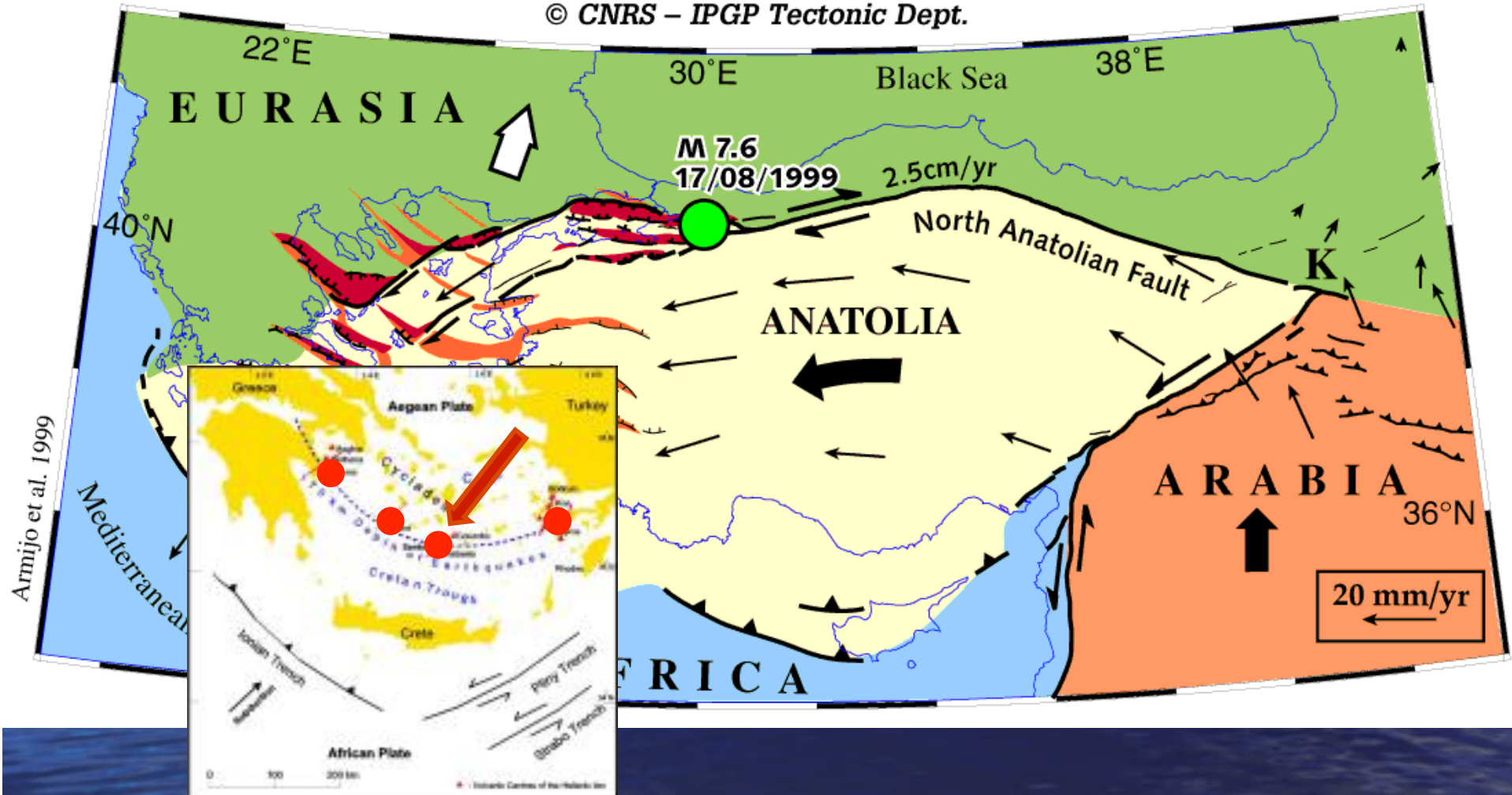
1866 eruption



GEODYNAMIC MODEL OF ANATOLIA-AEGEAN (Armijo et al 1996)

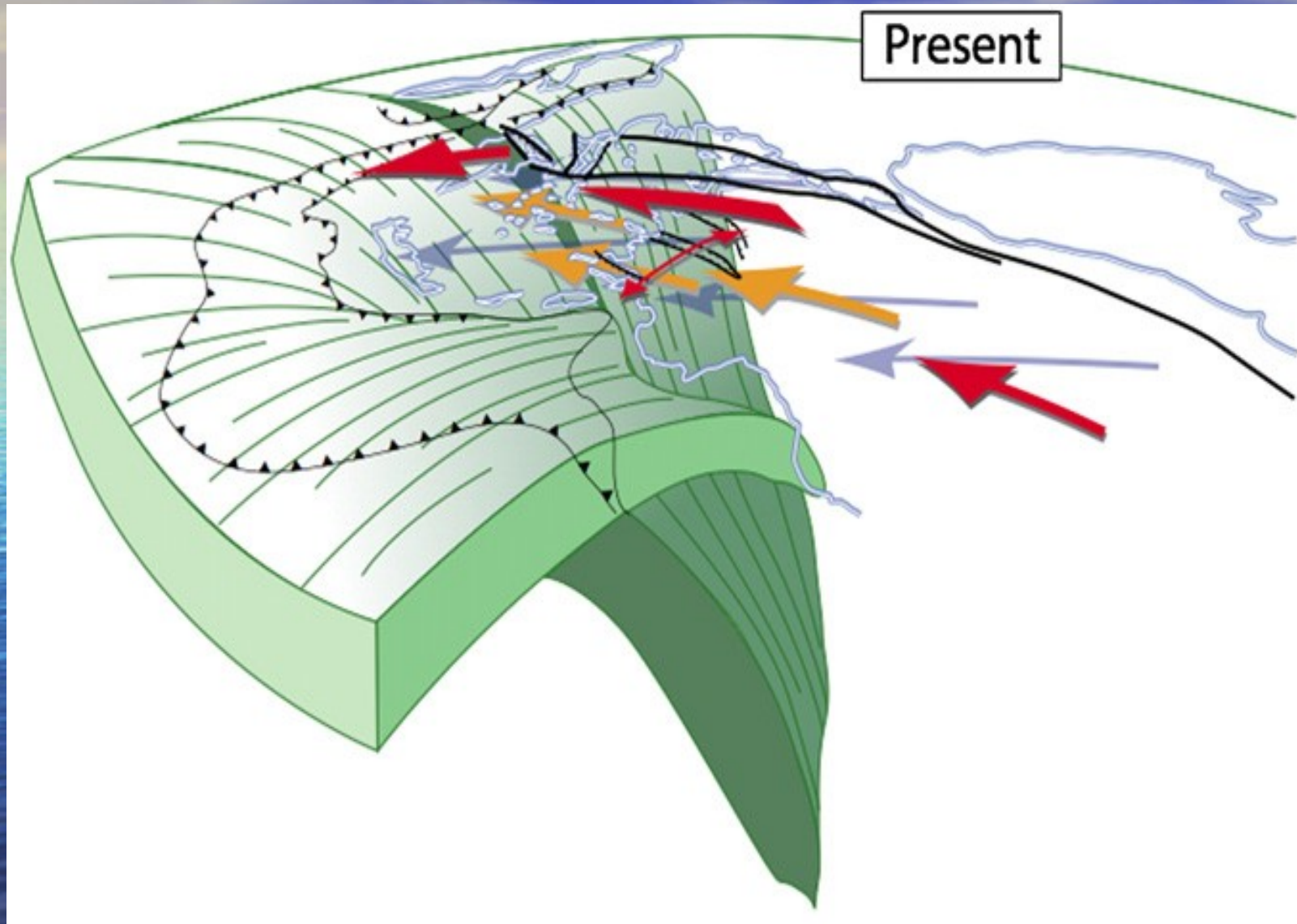
The volcanic arc is about 500 km long and 20 to 40 km wide and extends from the mainland of Greece through the islands of Aegina, Methana, Poros, Milos, Santorini, Kos, Yali, Nisyros and the Bodrum peninsula in Turkey

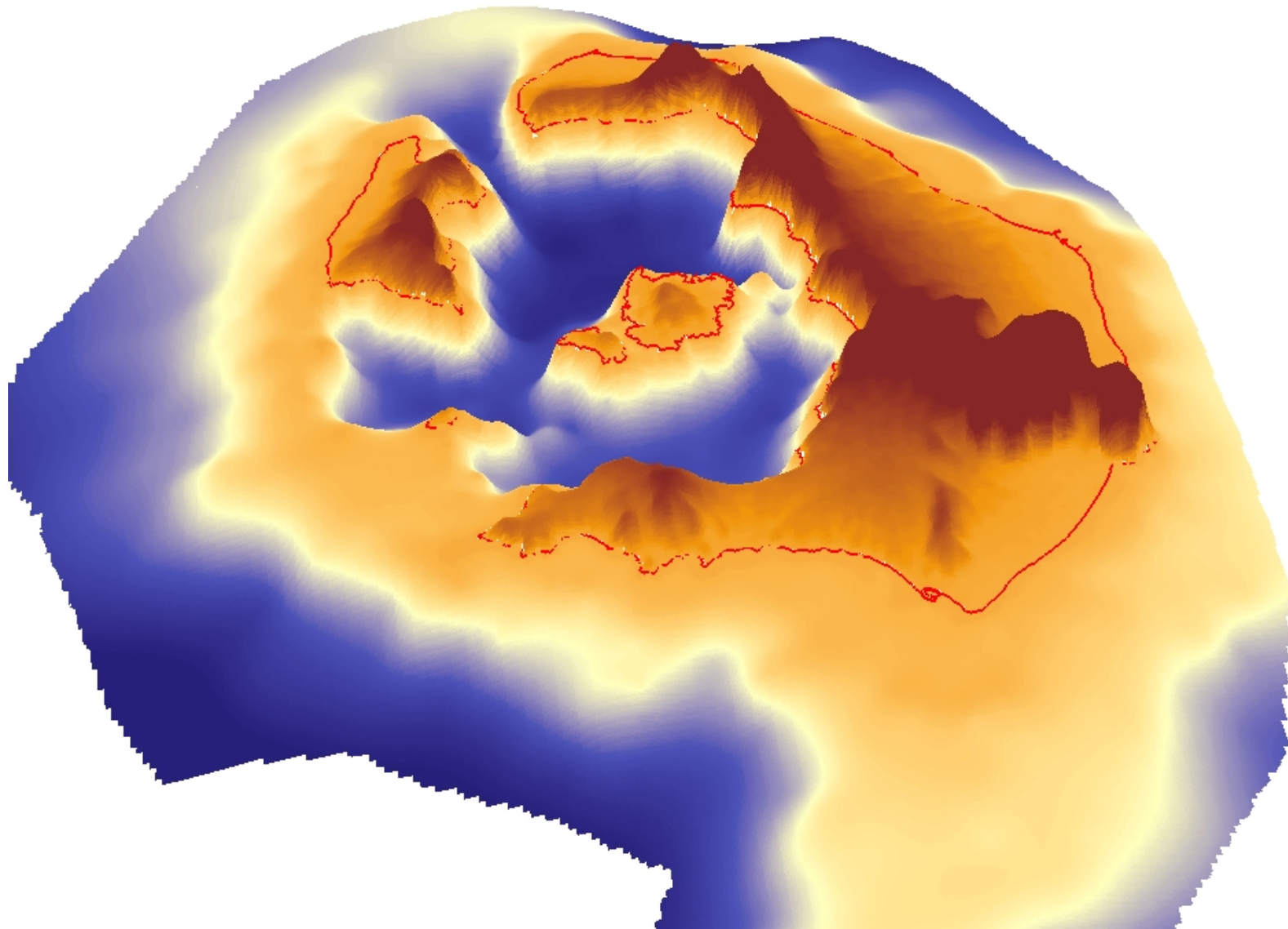
© CNRS – IPGP Tectonic Dept.



Westward movement of Anatolia. Thick arrows indicate relative movements, while thin ones indicate displacement vectors. (Armijo et al., 1996)

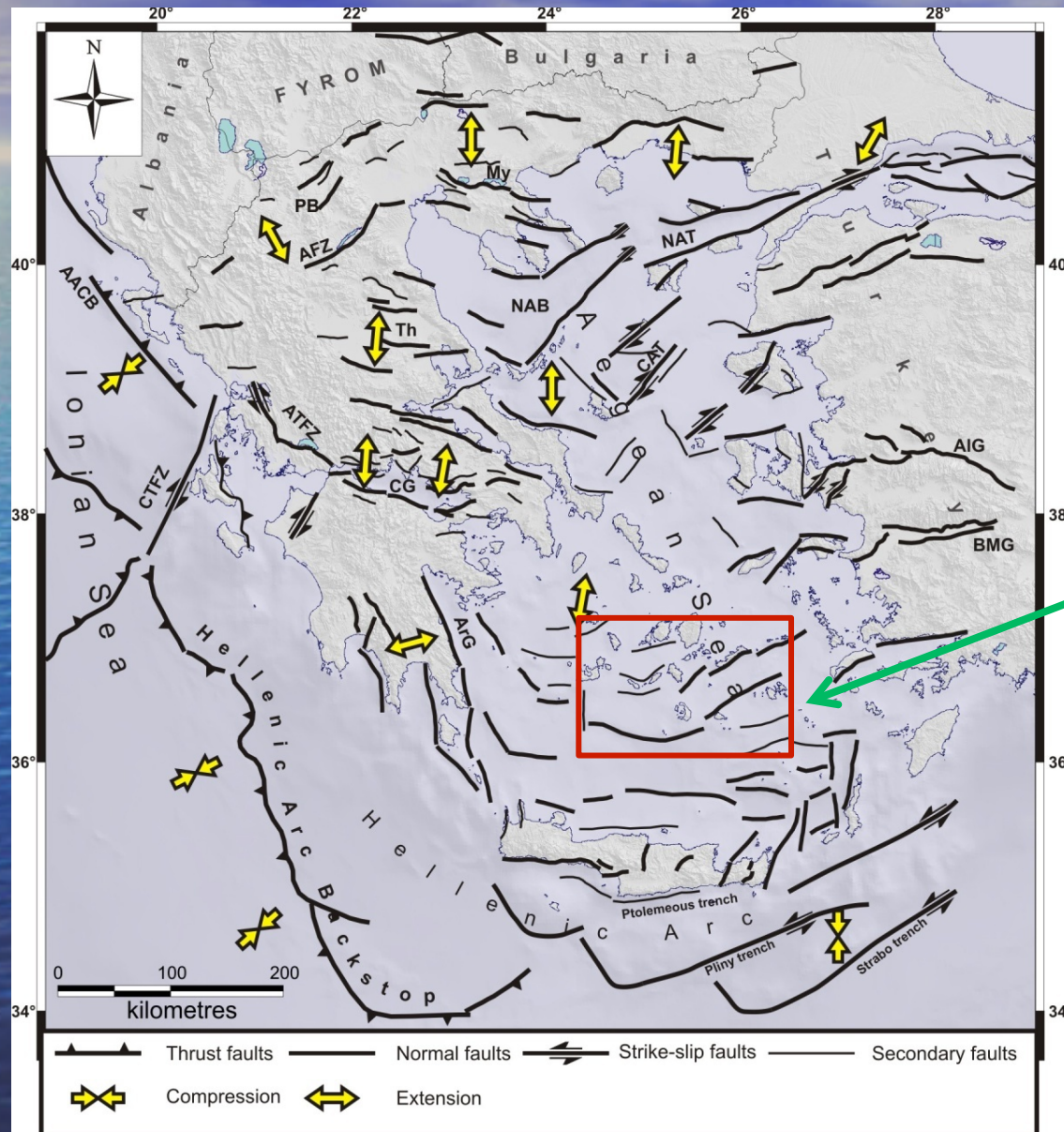
SUBDUCTION African Plate beneath Aegean



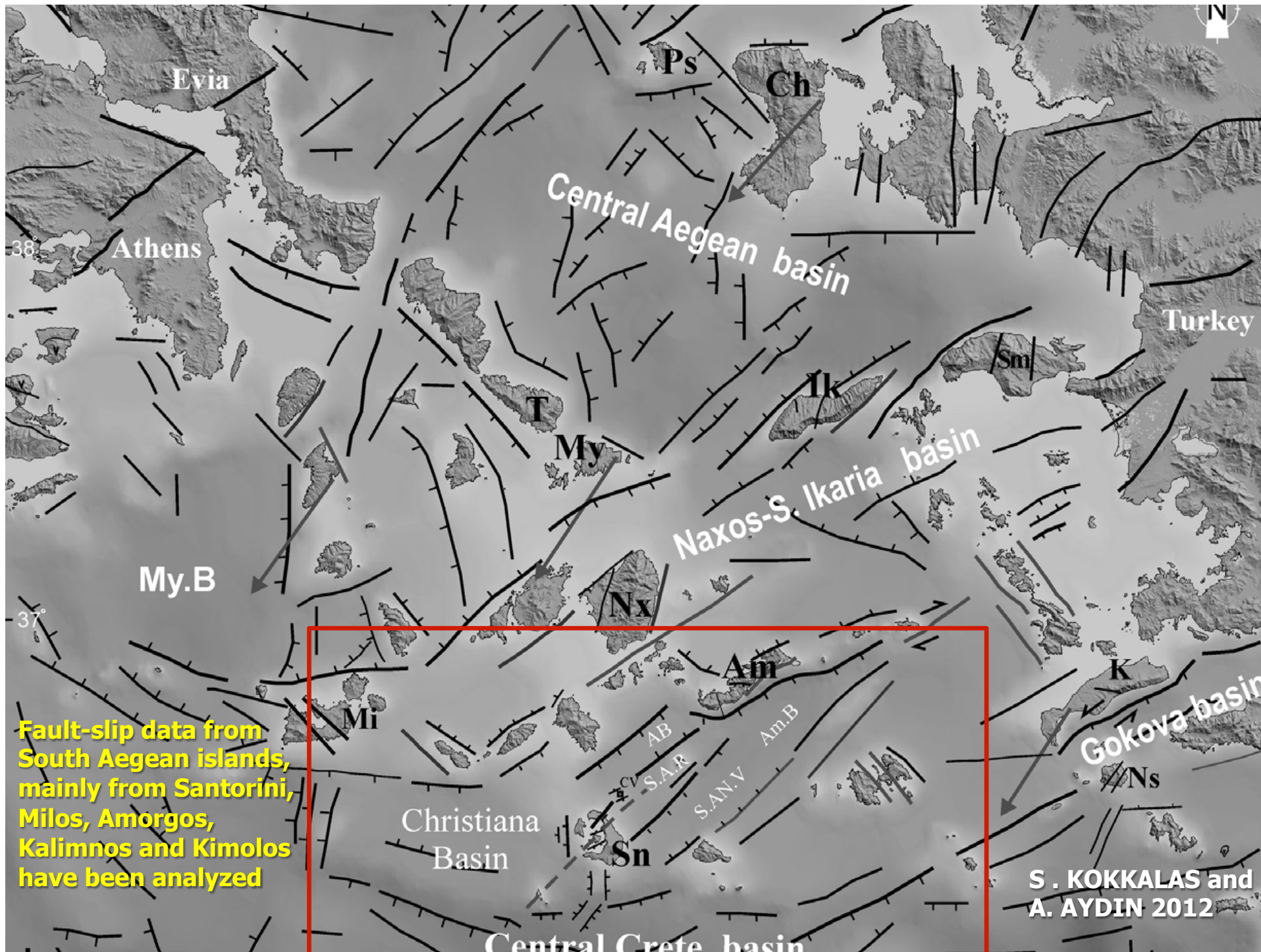


The new DEM of Santorini Volcano edifice, created by ASTER/GDEM (land), sea-floor topographic map (sea-floor depth) and Google Earth (present shoreline).

N-S trending σ_3 axis in the Aegean region



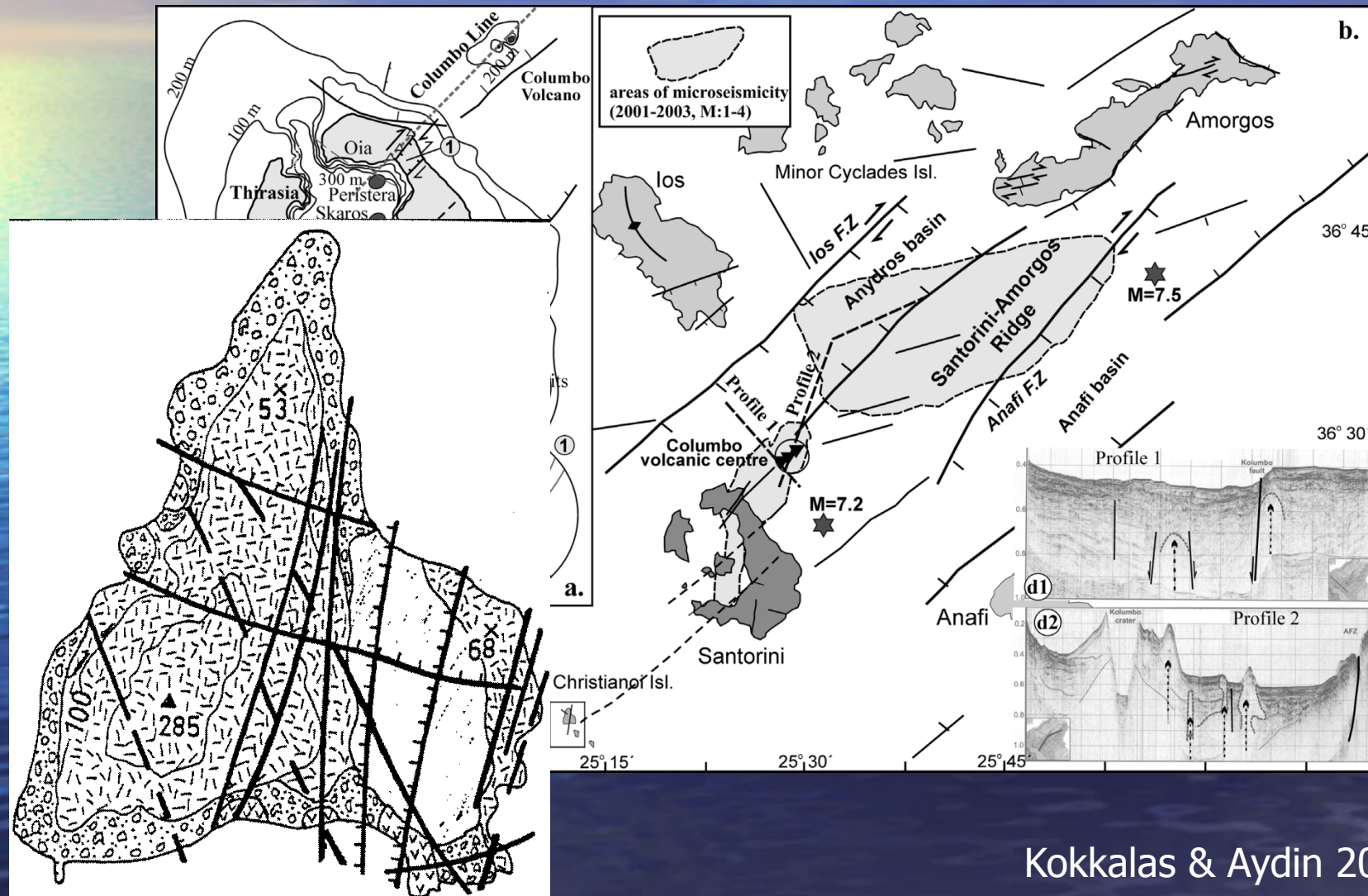
STUDY AREA



Fault-slip data from South Aegean islands, mainly from Santorini, Milos, Amorgos, Kalimnos and Kimolos have been analyzed

S. KOKKALAS and A. AYDIN 2012

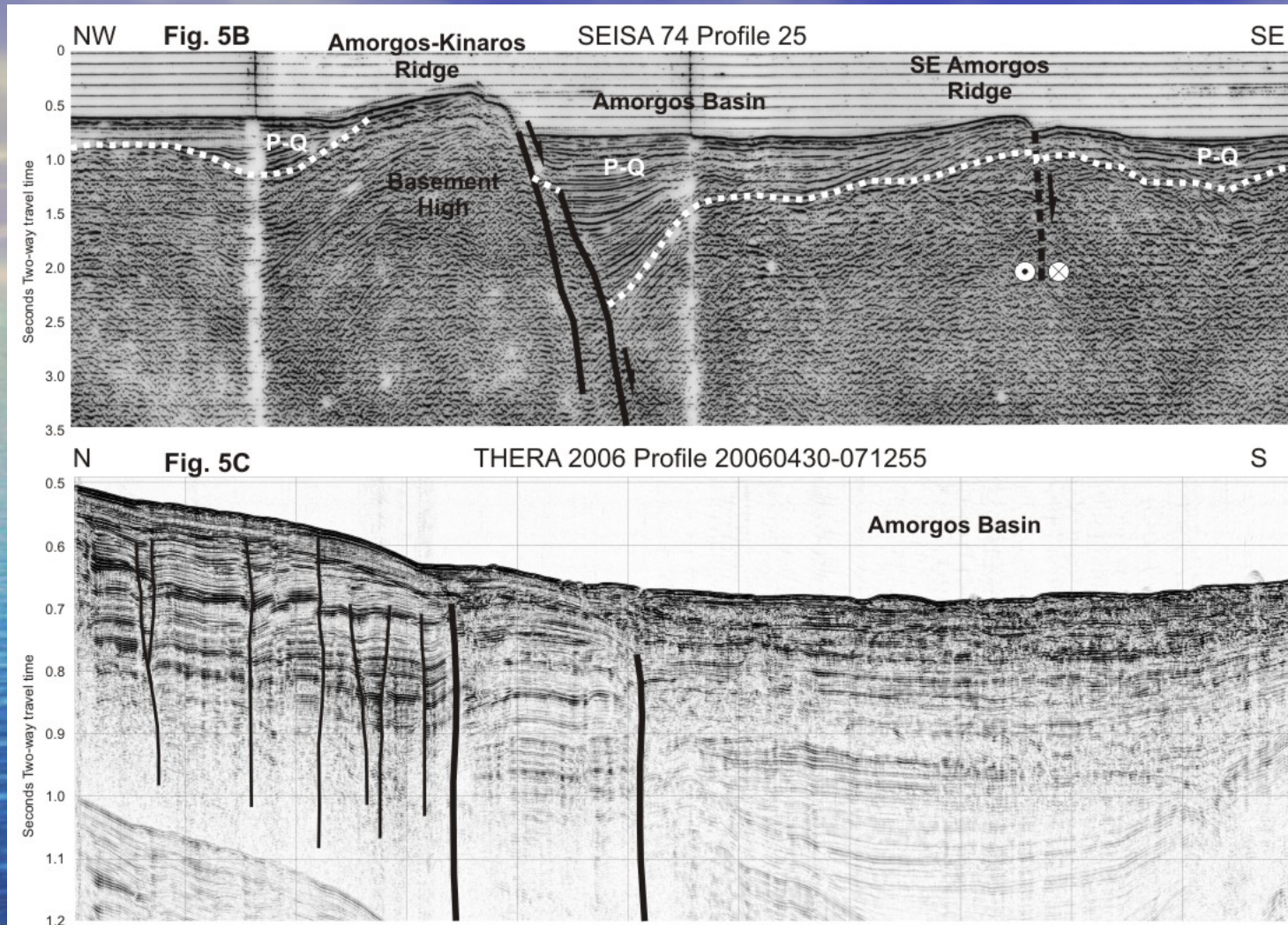
(a) Simplified tectonic map of the Santorini volcanic centre showing the distribution of dacite domes, cinder cones and submarine volcanoes with regard to the volcano-tectonic lineaments. Stereonet 1 displays fault slip data in the northern part of the island close to the Columbo line. (b) Map of the Santorini–Amorgos Fault Zone. Areas of higher earthquake activity (microseismicity) are marked by the two light grey shaded areas with dashed outline. (c) Inset shows fault pattern in the Christianoi Islands (modified from Mountrakis *et al.* 1998). (d1) Seismic reflection profile (profile 1 on map) across the Columbo submarine volcano (taken from Sakellariou *et al.* 2010). (d2) Composite seismic profile (profile 2 on map) along the Columbo volcano and Anydros basin (from Sakellariou *et al.* 2010). The bright spot area below volcano caldera suggests the presence of fluids or gas about 200 m beneath the caldera.



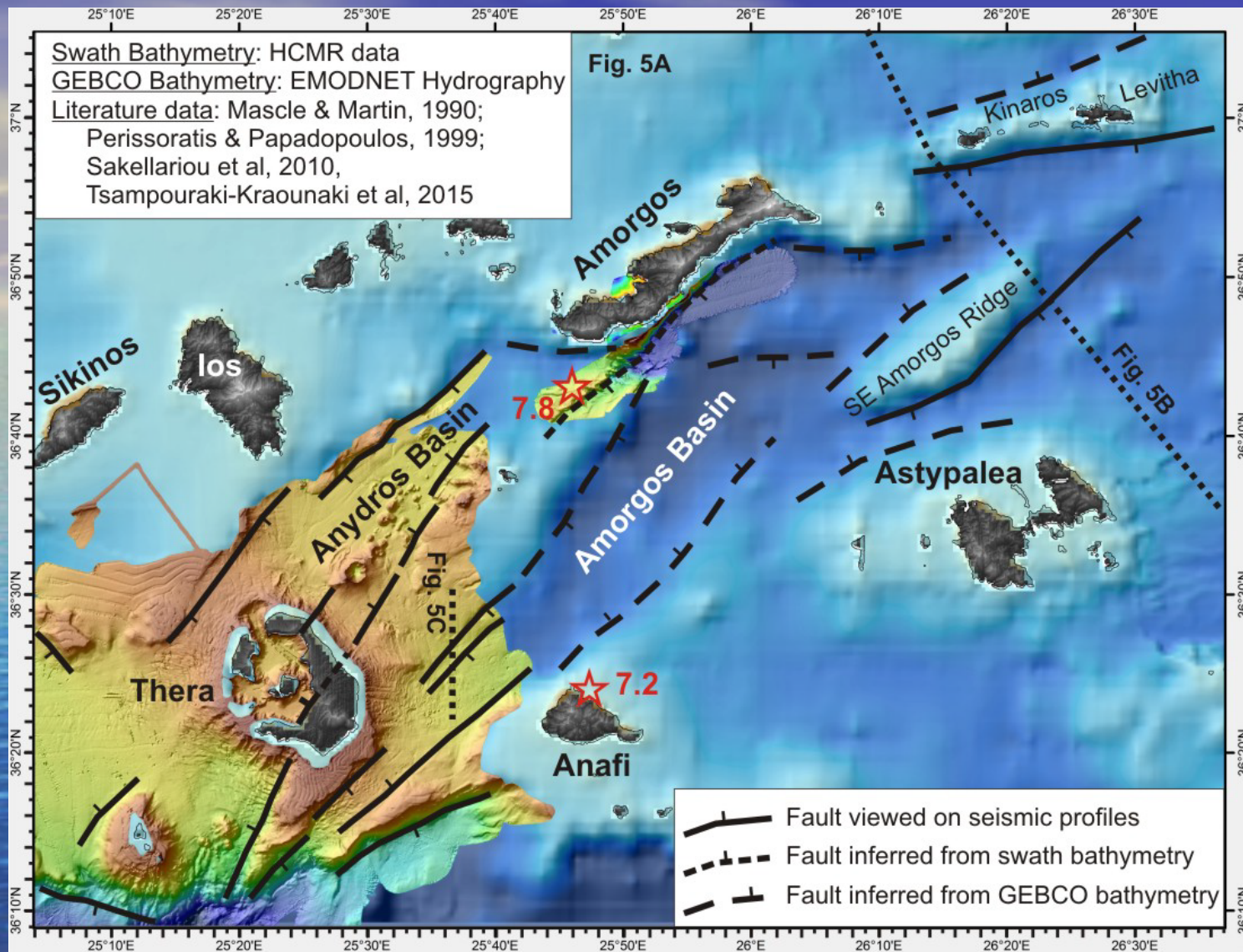
AMORGOS fault



Hozoviotissa monastery on the
fault surface (wall)

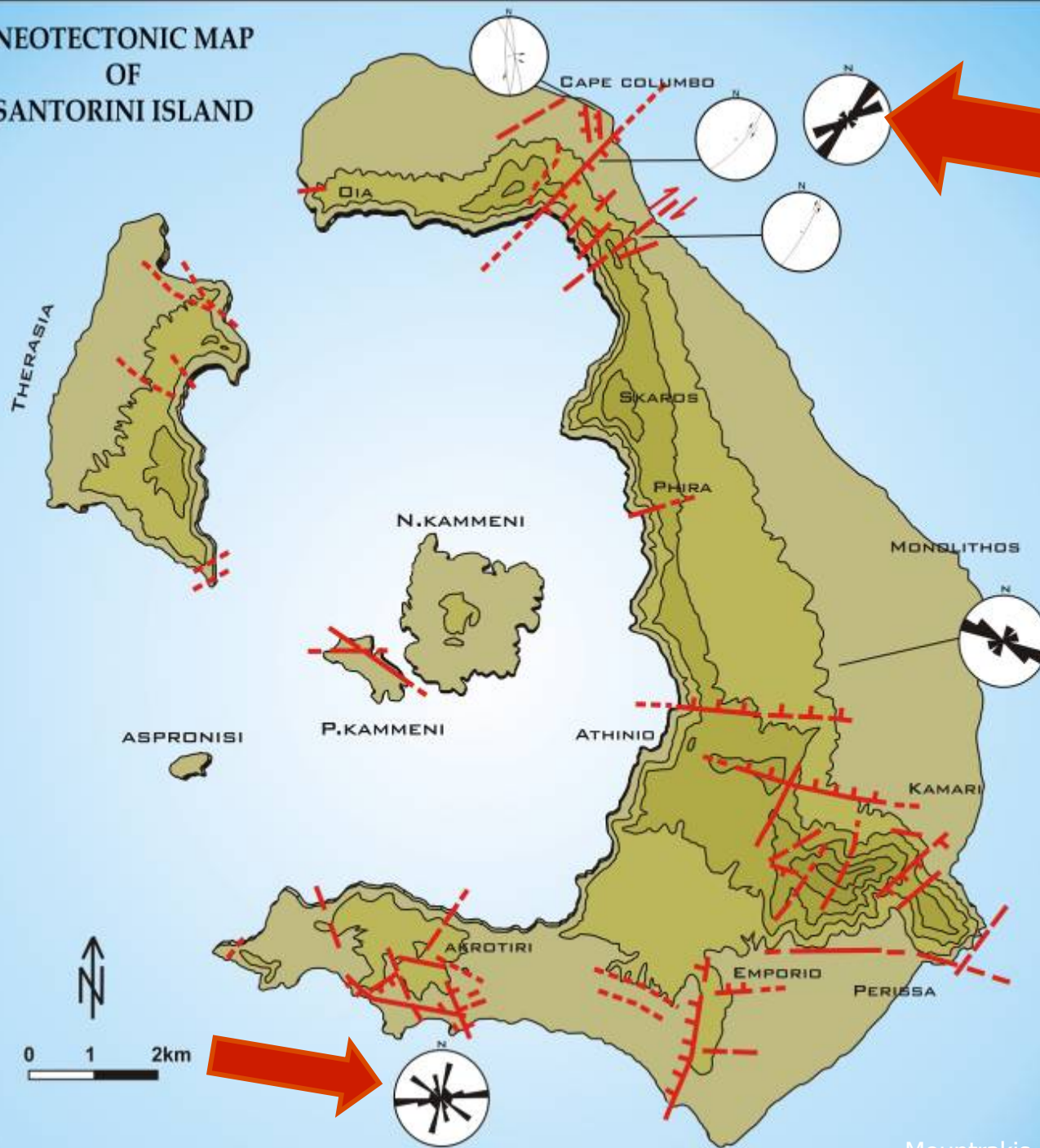


**SEISA multi-channel Line 25 (Masle & Martin, 1990).
 C: Single channel HCMR profile (Sakellariou et al, 2010).**



DEM and faults of Santorini-Amorgos area. Red stars show the epicenters of the 1956 Amorgos earthquakes. (Sakellariou D and Tsampouraki-Kraounaki 2016)

NEOTECTONIC MAP OF SANTORINI ISLAND



Submarine
Columbo
volcano

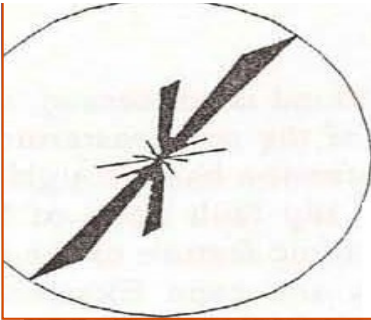
Three-dimensional model of
the current morphology of
the Kolumbo volcano

500 m-deep
crater, 18 m
below sea
level

Santorini,
Thera or
Strogyle
island
complex

Columbo conjugate normal faults

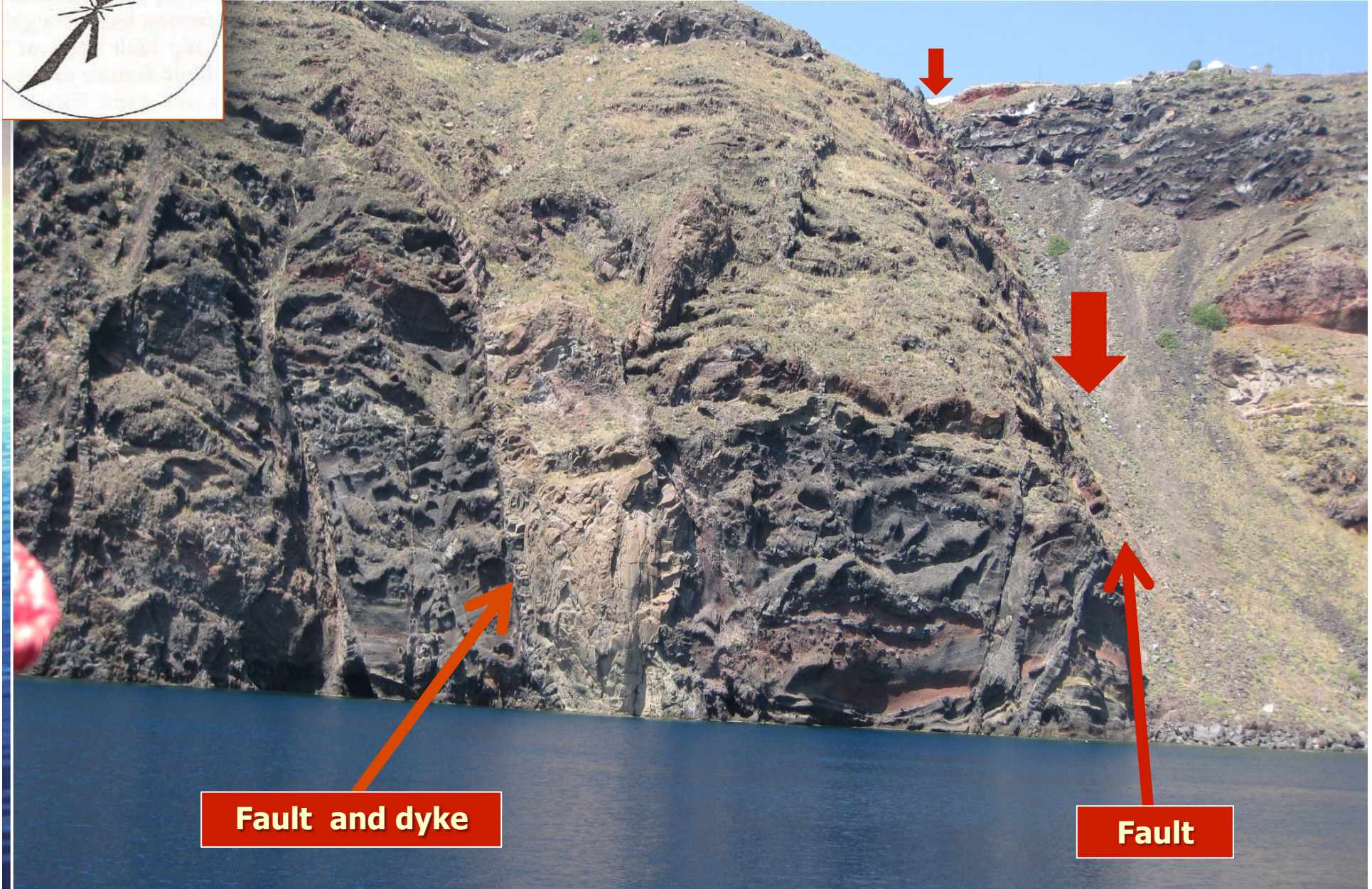
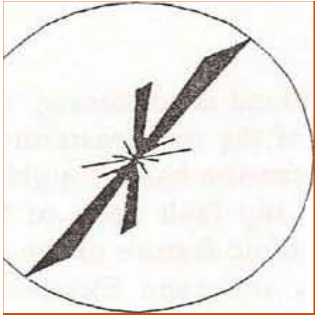




**Fault
and
dyke**



NE-SW trending FAULTS and DYKES



Fault and dyke

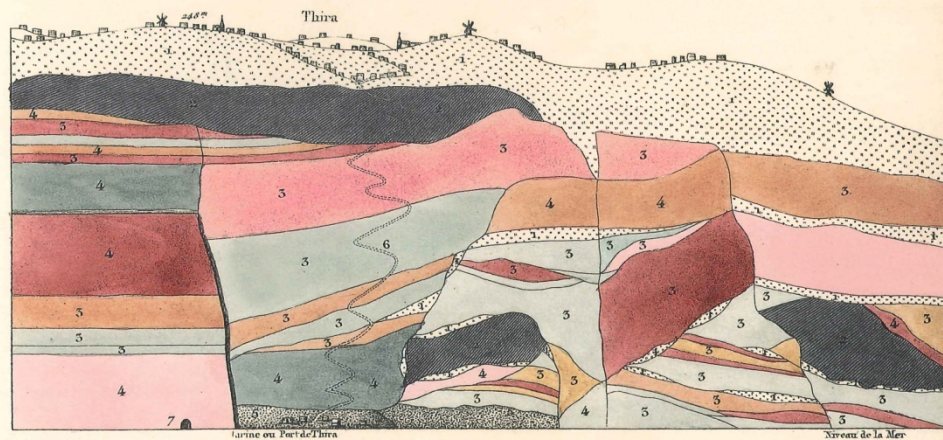
Fault

The Fira fault

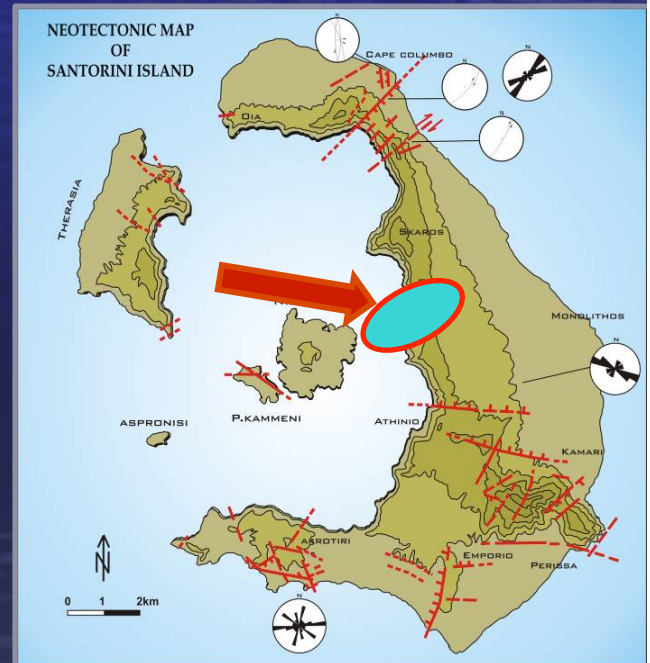
through the France expedition de Moree (1829-38) to modern scientific approach.

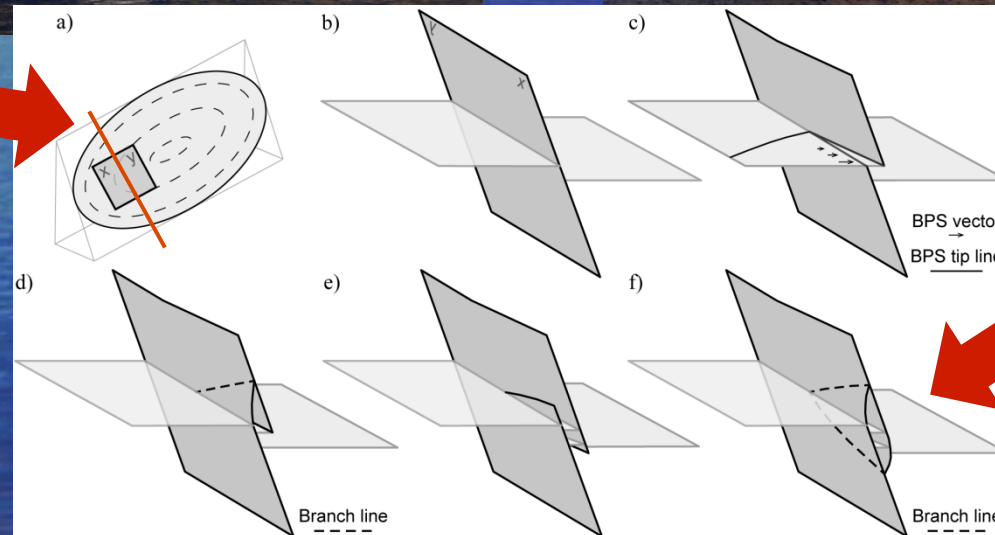
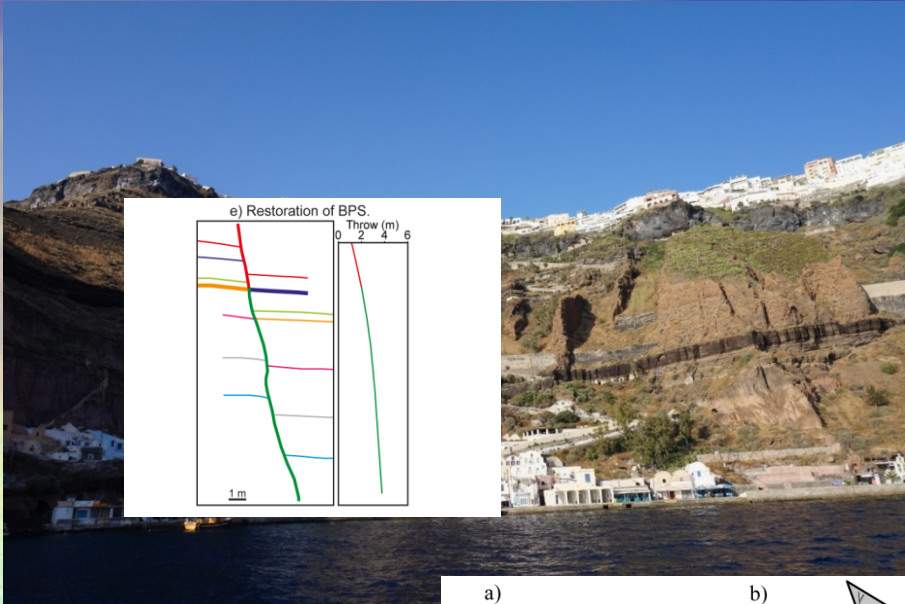


Fig. 4. VUE D'UNE PARTIE DE L'ESCARPEMENT DE SANTORIN AU PORT DE THIRA.
par M. Virlet.



- | | |
|---|--|
| 1. Agglomérats trachytiques et ponces blancs. | 4. Agglomérats trachytiques en bancs épais. |
| 2. Concrètes de trachytes. | 5. Tufes de Débris variés. |
| 3. Agglomérats trachytiques en zones multiples. | 6. Chemins en Zig-zag qui conduit de la ville au port. |
| 7. Magasins ou Caves creusés dans le Conglomérat. | |

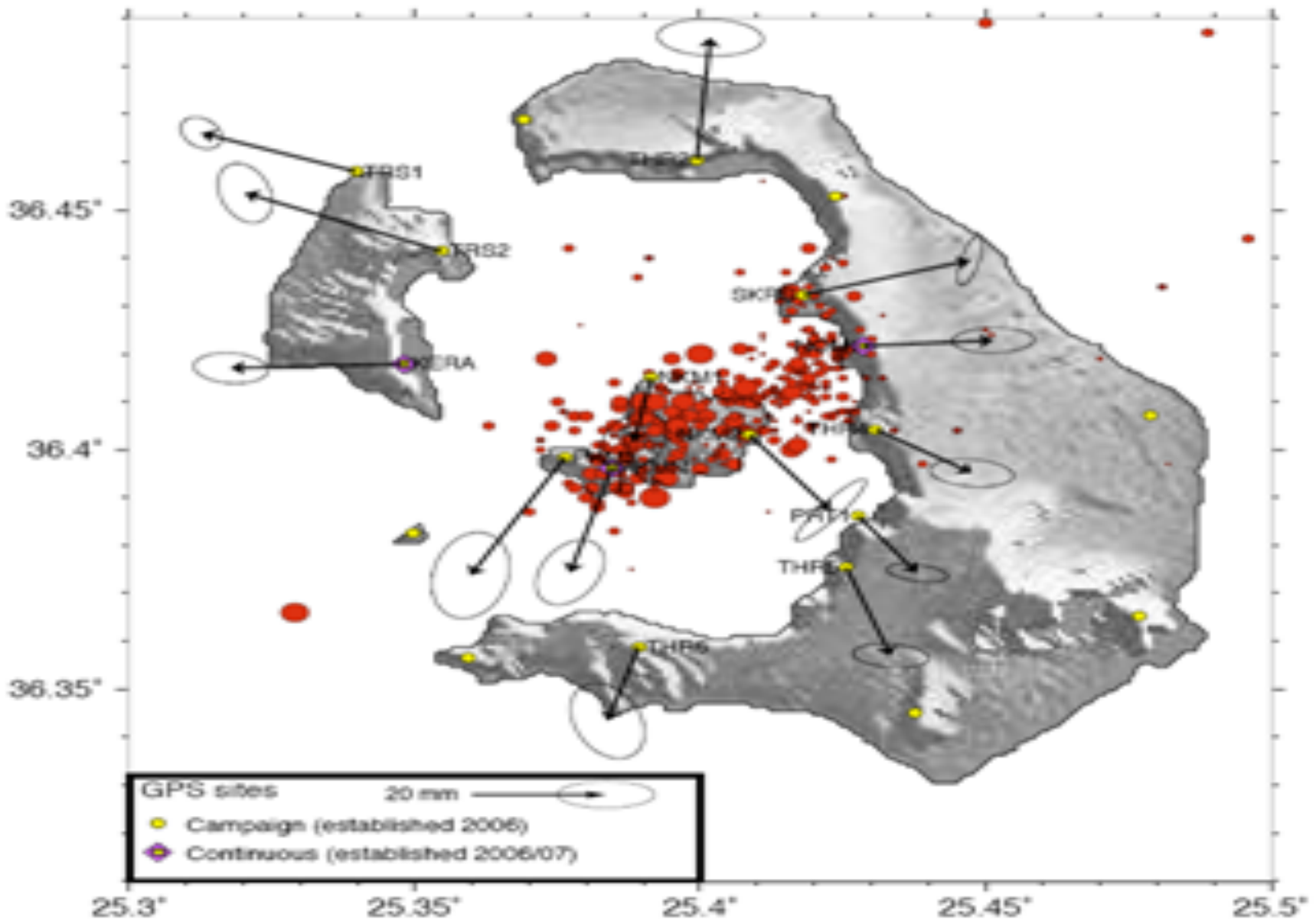




a) An ideal elliptical normal fault surface showing fault displacement contours (dashed lines) and tip-line (solid line), in propagation of both fault segment and the formation of a relay zone which with increased displacement the two fault segments form a fault bounded lens (f) encloses a repeated part of the sequence, within an otherwise continuous fault surface.

- The Fira (Phera) fault is a Normal Fault trending ENE-WSW.
- It is a “segment” of subparallel structures of a longer “fault zone”, including the known volcanic centers and the 1956 earthquake great Amorgos-Thera fault.
- It shows gradually smaller Displacement from the sea level to top lava layer (*Nomikos Conference Center*). Syn-volcanic fault growth.
- It's internal structure is complex (*under investigation*).
- It's known fault length corresponds to weak or moderate earthquake.

Projected displacement field from 2010–2011 GPS campaigns



Known fault length (seismogenic segment) ~6 km



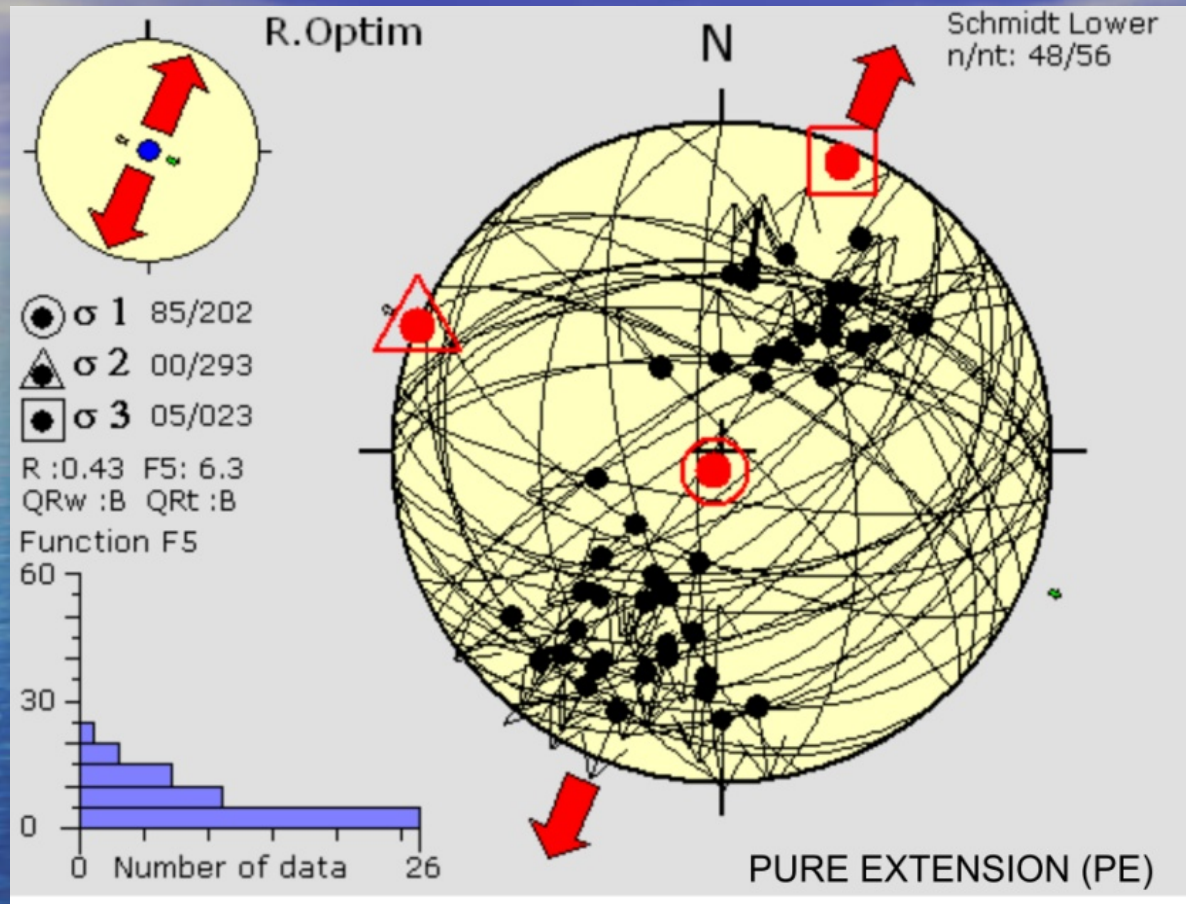
FAULT LENGTH

Known : **5 - 6 km**

Unknown : $6+5+5 =$ **16 km or longer**

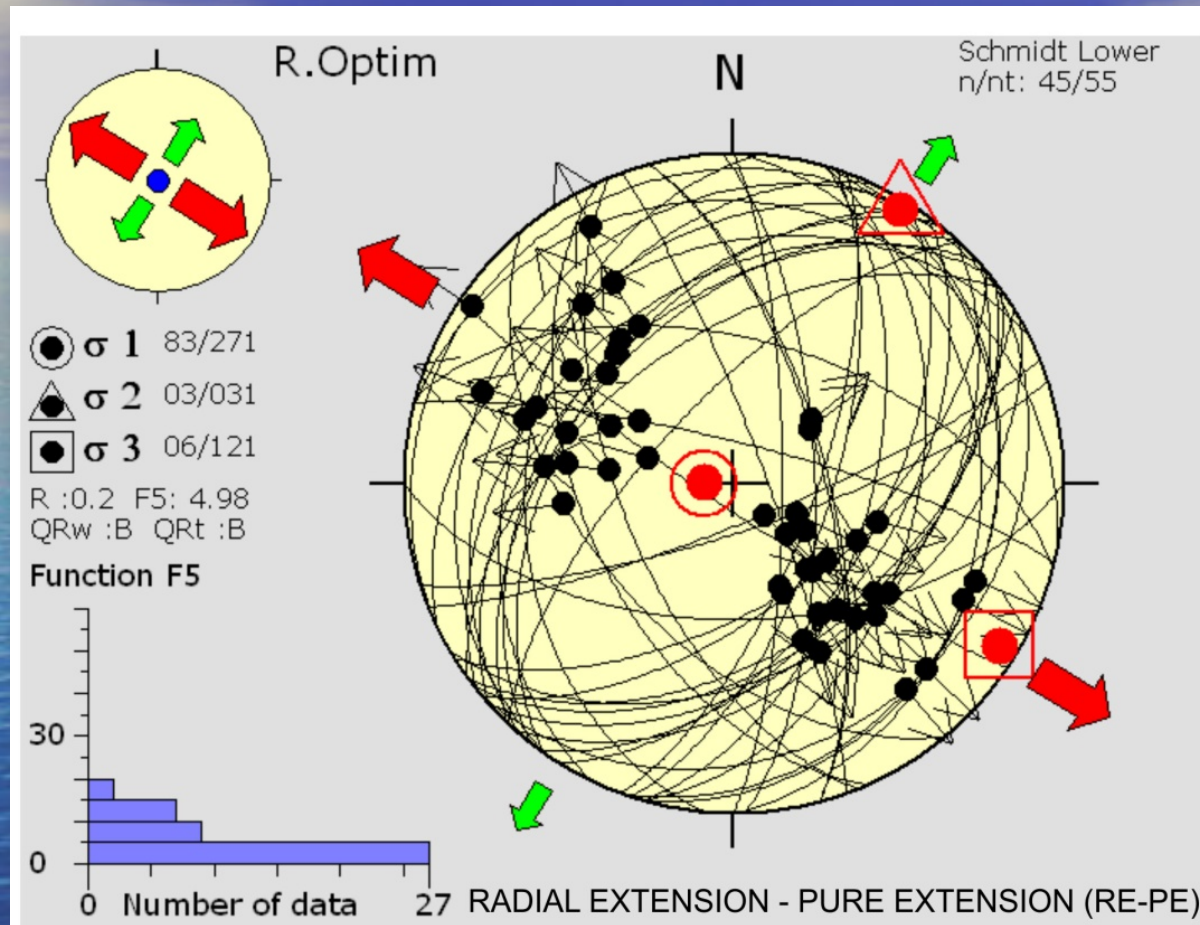


NE-SW Oblique-slip high angle extensional Faults and E-W dip-slip low angle normal fault

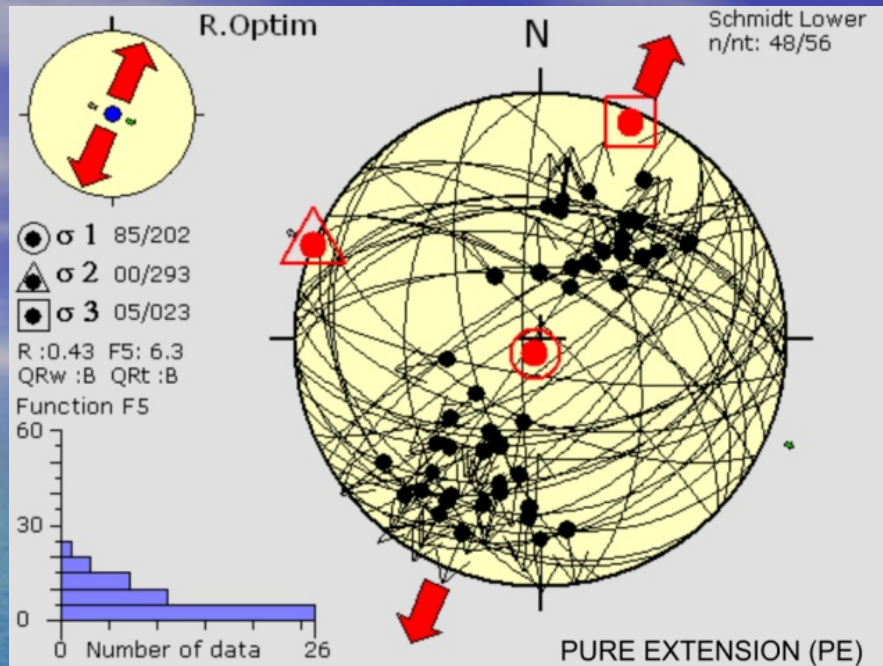


The stress inversion method applied on these fault-slip data and on doing this we use the software Win-Tensor 3.0 as provided by Delvaux, 2011).

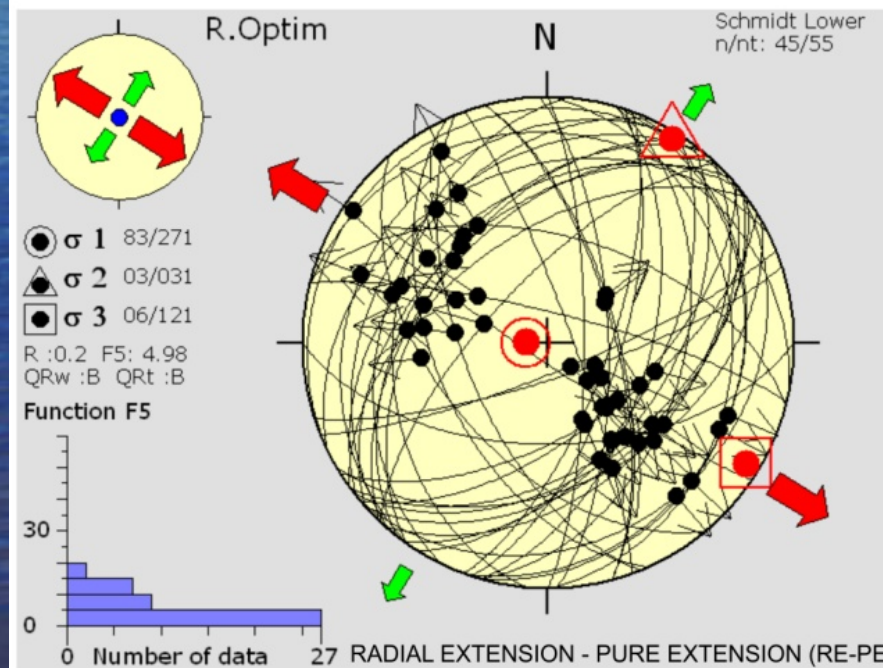
NE-SW normal faults low angle mainly



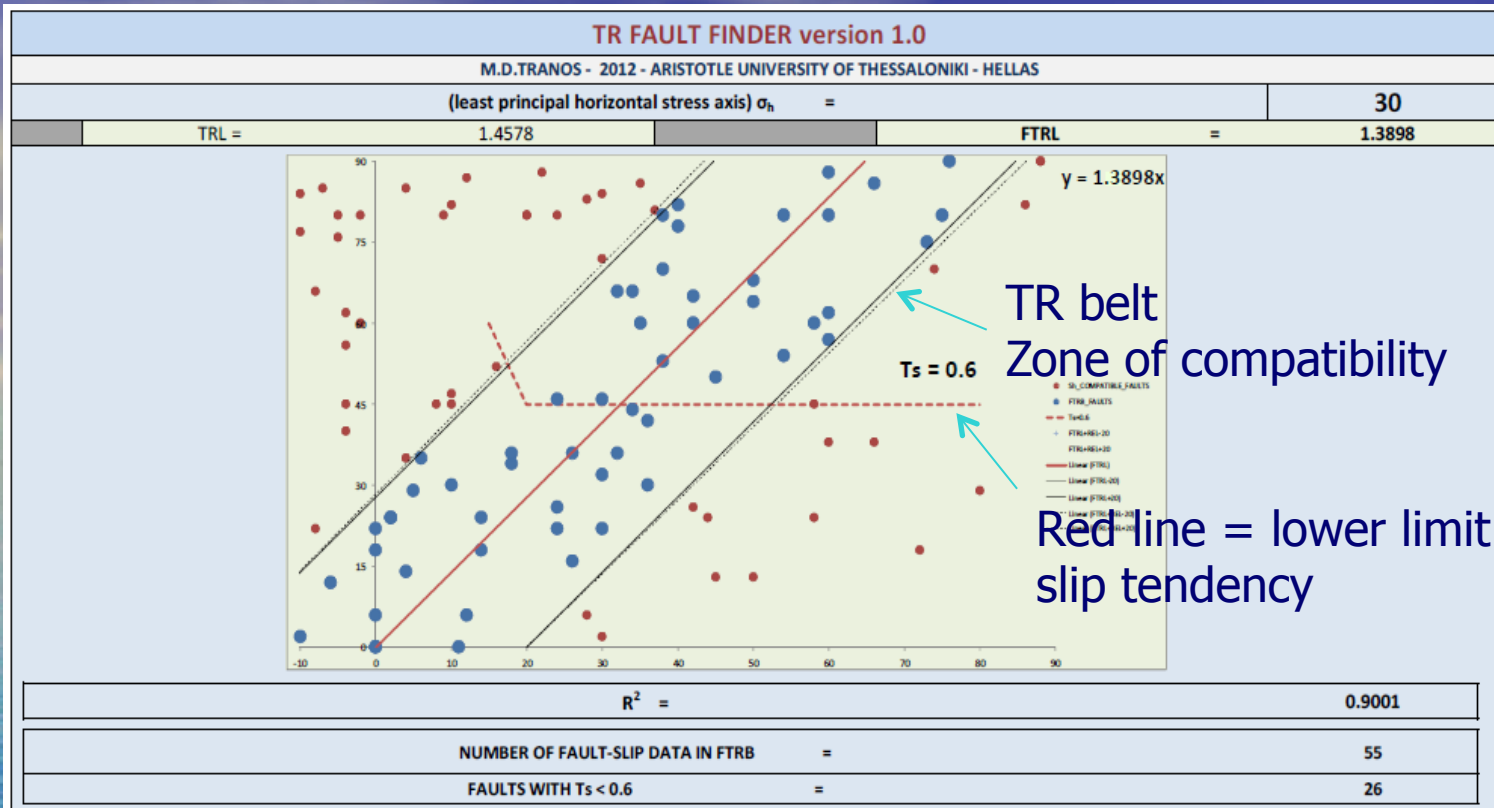
The stress inversion method of fault-slip data and on doing this we use the software Win-Tensor 3.0 as provided by Delvaux, 2011).



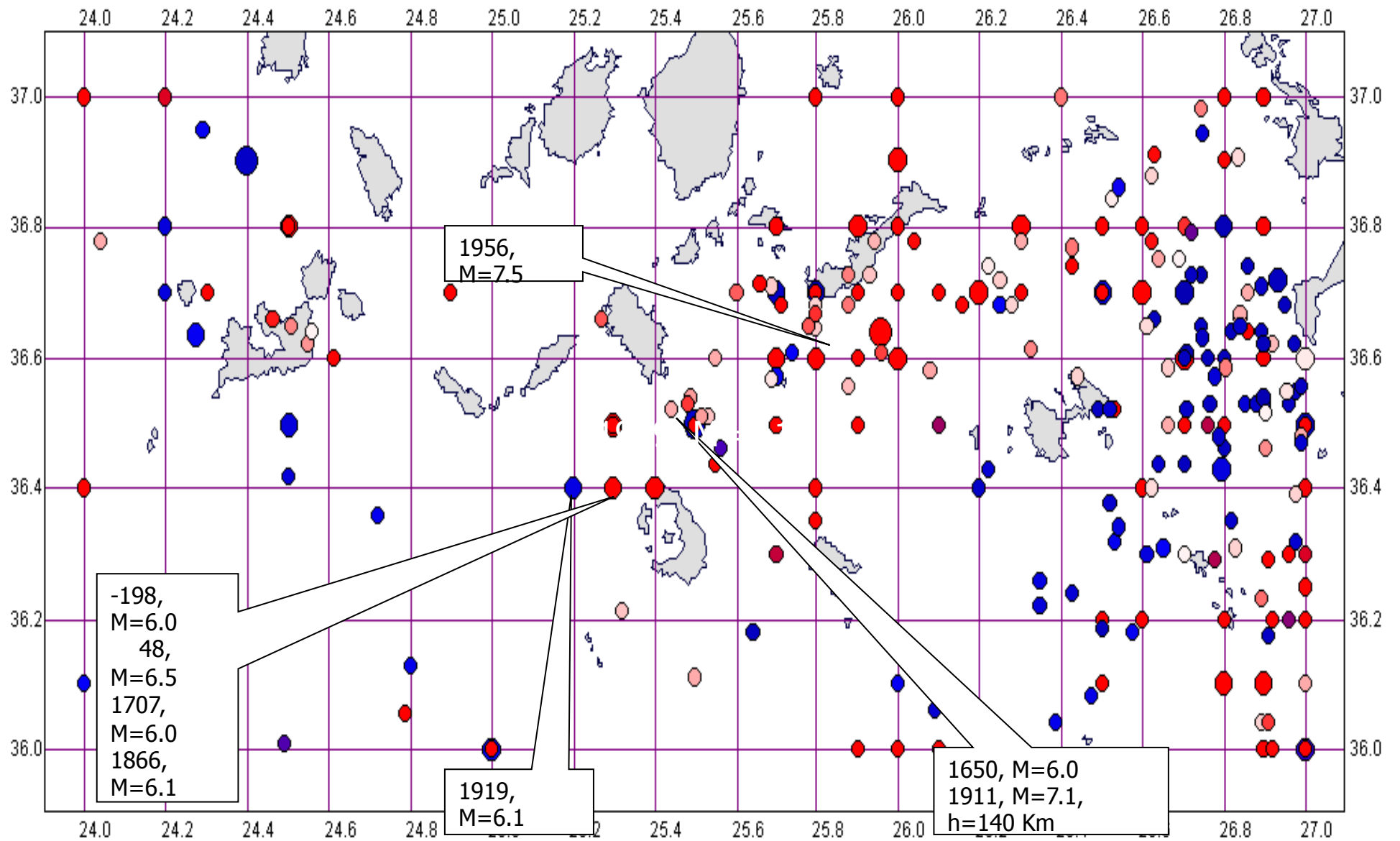
a) Extension with
 σ_1 : 202°-85°,
 σ_2 : 293°-00°,
 σ_3 : 023°-05°
 and stress ratio
 R = 0.42



b) the second
 Extension
 σ_1 : 271°-83°,
 σ_2 : 031°-03°,
 σ_3 : 121°-06°
 stress ratio R = 0.2.



| A/A | LABEL | SD(PT90-A) | [(Sh-FTDIPD)] | $T_s < 0.6$ | FT_DIPD | FT_DIPA | L_TREND | L_PLUNGA | PITCH | SOS | COMMENTS |
|-----|---------|------------|---------------|-------------|---------|---------|---------|----------|-------|-----|----------|
| 3 | SAN_003 | 26 | 16 | | 46 | 86 | 324 | 64 | | NS | |
| 11 | SAN_011 | 42 | 60 | SAN_011 | 270 | 44 | 219 | 31 | | NS | |
| 12 | SAN_012 | 76 | 90 | SAN_012 | 300 | 48 | 219 | 10 | | NS | |
| 13 | SAN_013 | 18 | 34 | | 176 | 60 | 209 | 55 | | ND | |
| 18 | SAN_018 | 66 | 86 | SAN_018 | 304 | 88 | 33 | 24 | | ND | DD |
| 19 | SAN_019 | 60 | 80 | SAN_019 | 310 | 74 | 31 | 29 | | ND | DD |
| 20 | SAN_020 | 50 | 64 | SAN_020 | 326 | 86 | 53 | 40 | | ND | |
| 23 | SAN_023 | 18 | 36 | | 174 | 58 | 206 | 54 | | NS | |
| 25 | SAN_025 | 32 | 66 | SAN_025 | 144 | 68 | 203 | 52 | | ND | |
| 28 | SAN_028 | 12 | 6 | | 24 | 52 | 43 | 50 | | ND | NN |
| 29 | SAN_029 | -10 | 2 | | 208 | 64 | 230 | 62 | | ND | NN |
| 31 | SAN_031 | 24 | 22 | | 8 | 42 | 39 | 38 | | ND | |
| 40 | SAN_040 | 60 | 88 | SAN_040 | 298 | 36 | 233 | 17 | | NS | |
| 44 | SAN_044 | 40 | 82 | SAN_044 | 128 | 30 | 172 | 23 | | ND | |
| 45 | SAN_045 | 54 | 80 | SAN_045 | 130 | 58 | 199 | 30 | | ND | |



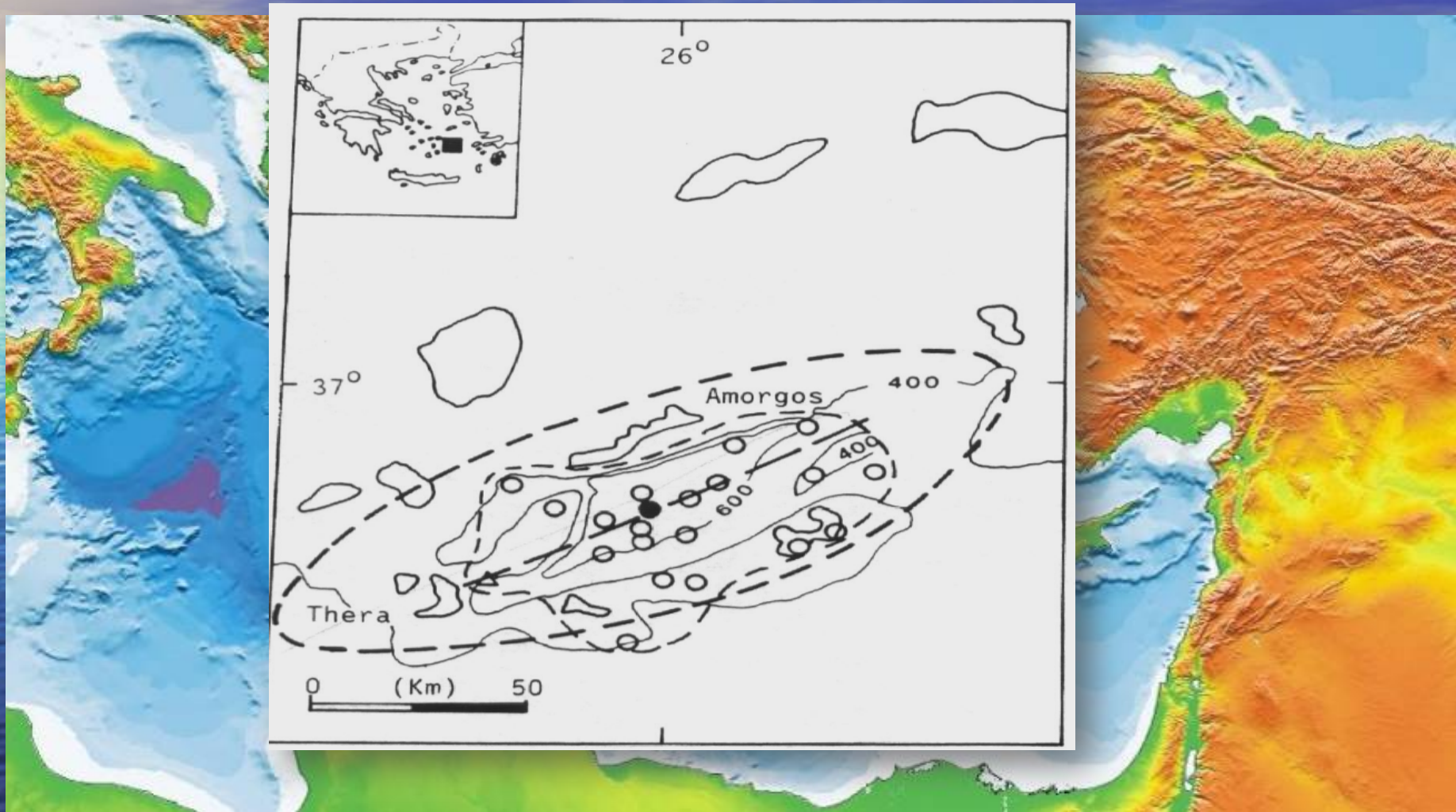
MEAN RETURN PERIOD OF STRONG EARTHQUAKES

Μέση Περίοδος Επανάληψης Σεισμών στην Ευρύτερη περιοχή της Σαντορίνης

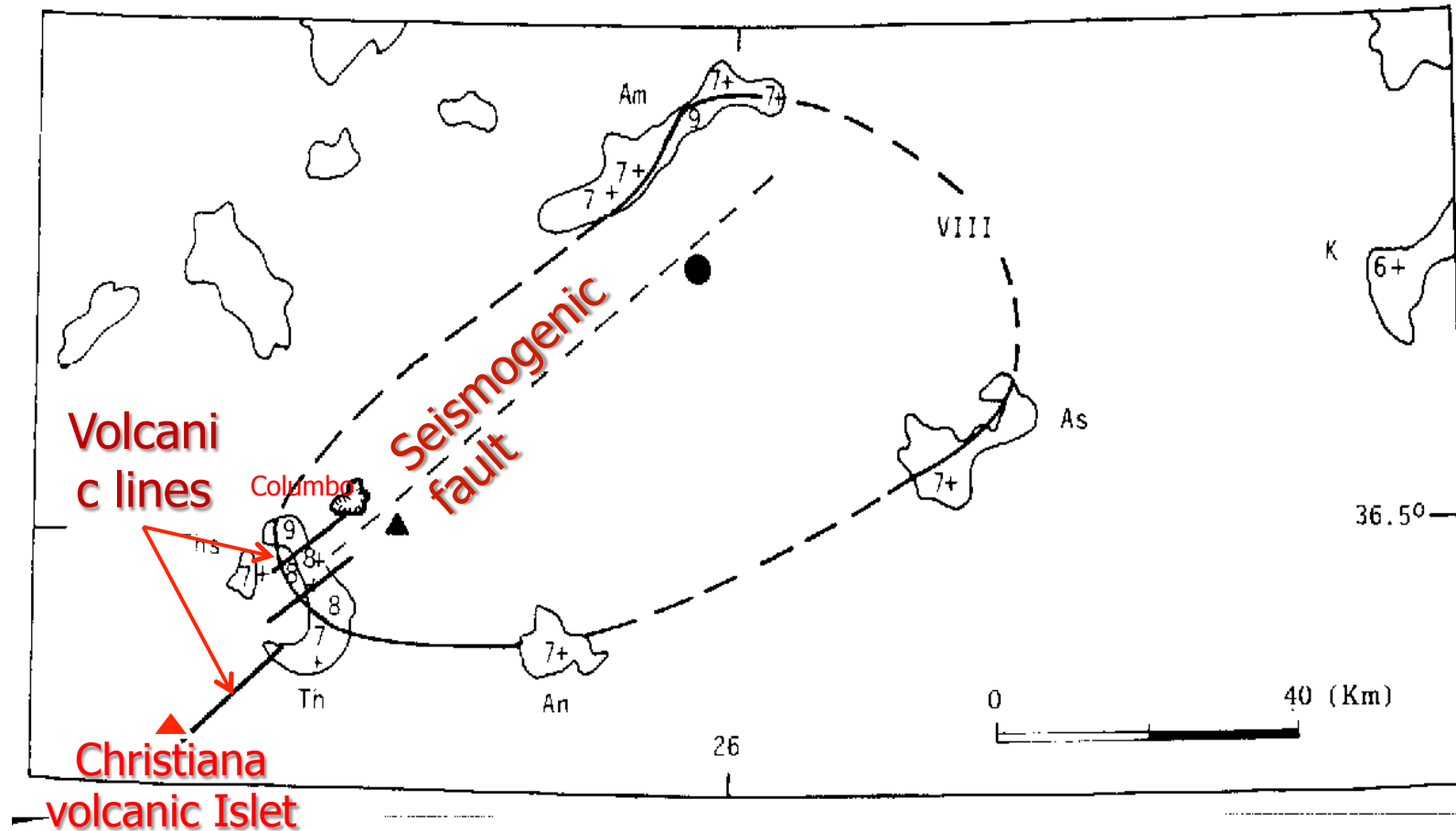
TM

| ❖ Magnitude | Tm |
|--------------|------------------|
| ❖ 6.0 | 15 (yrs) |
| ❖ 7.0 | 97 (yrs) |
| ❖ 7.5 | 250 (yrs) |

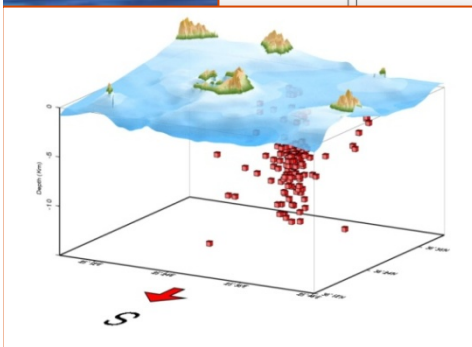
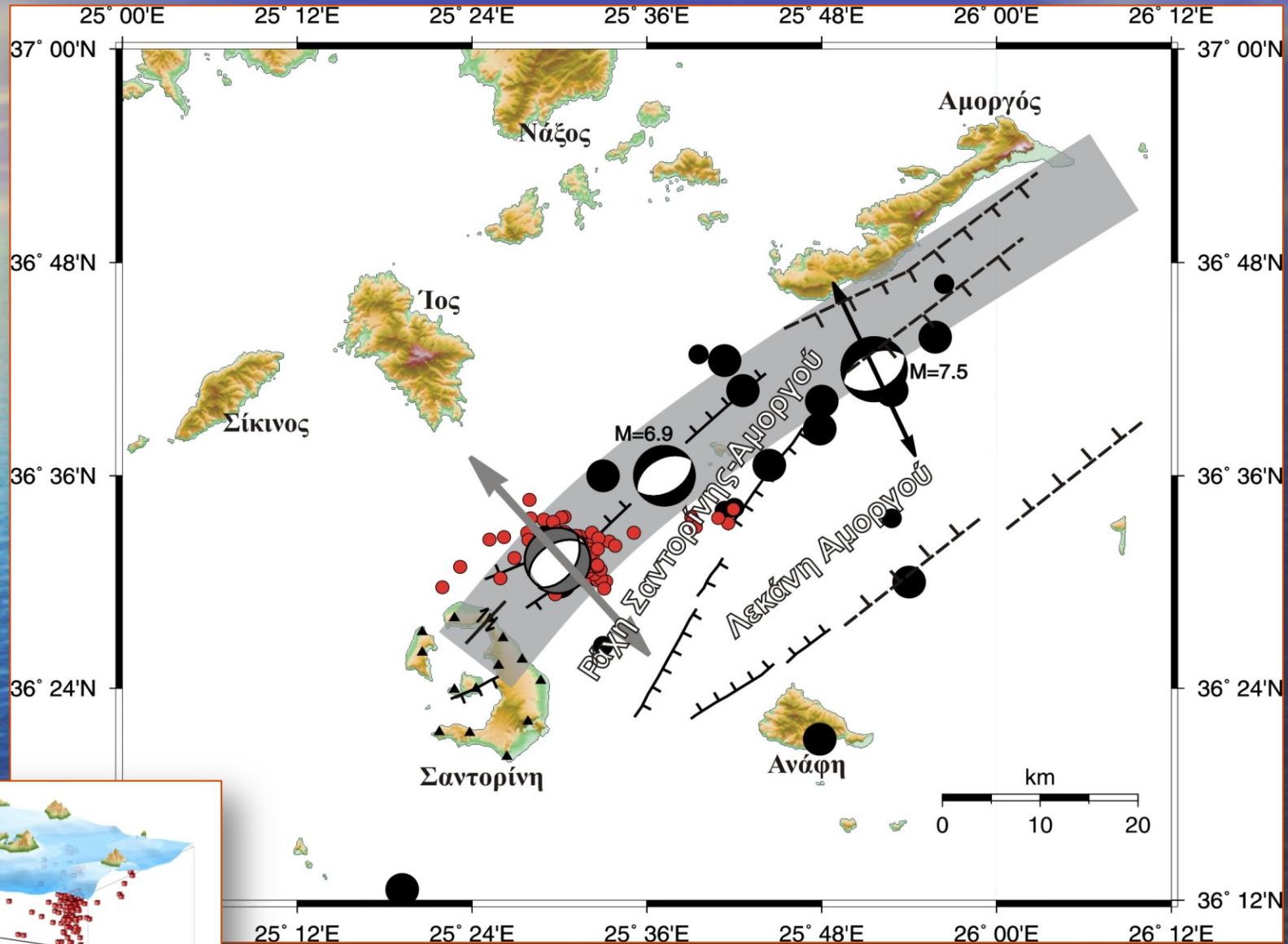
SANTORINI AMORGOS NEOTECTONIC PATTERN AND THE 1956 $M_s=7.5$ EARTHQUAKE (Amorgos Trough - Santorini volcanic activity, South Aegean sea



The 1956 earthquake intensities on the main tectonic lines



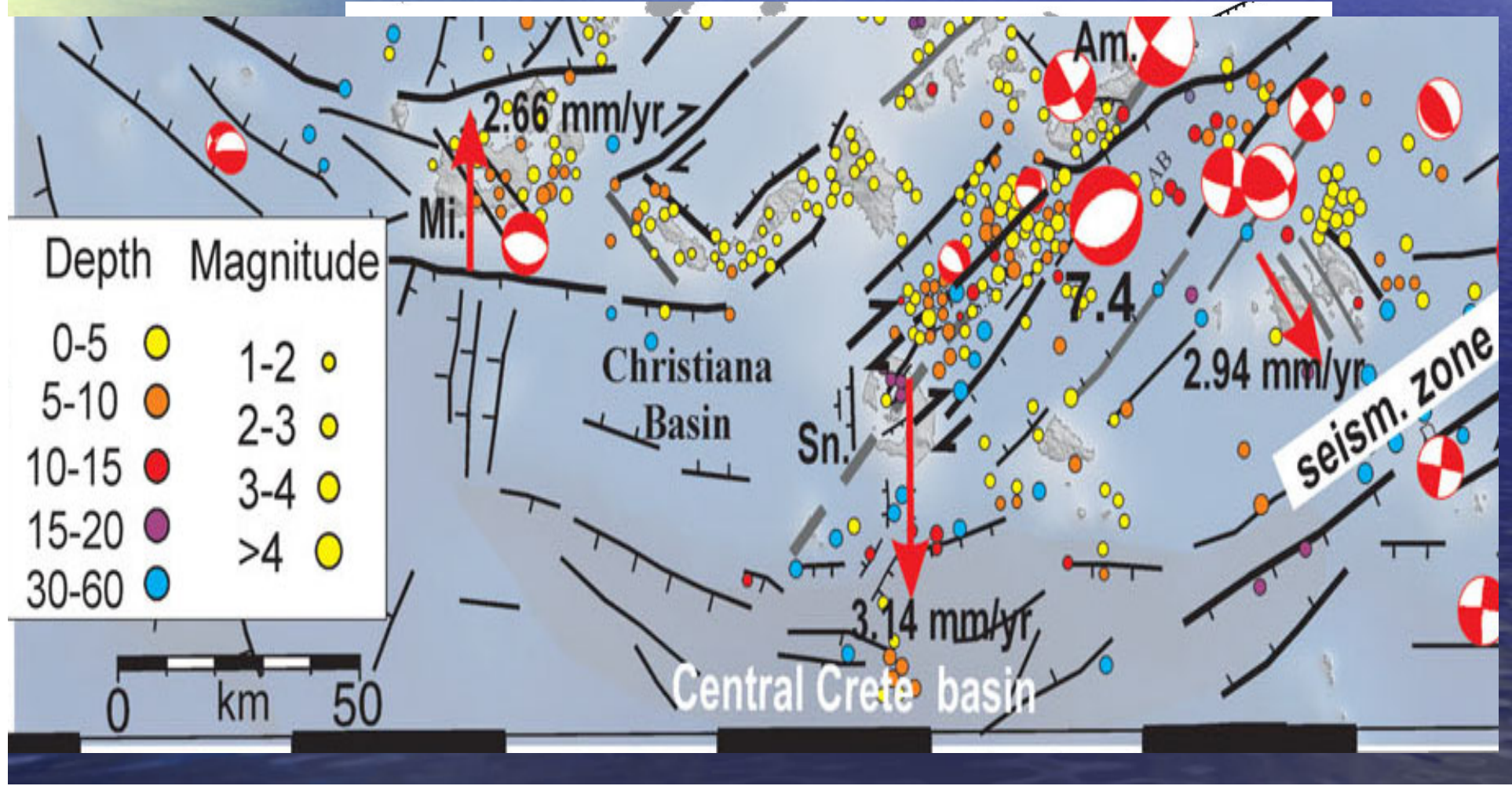
SEISMOTECTONICS OF SANTORINI-AMORGOS



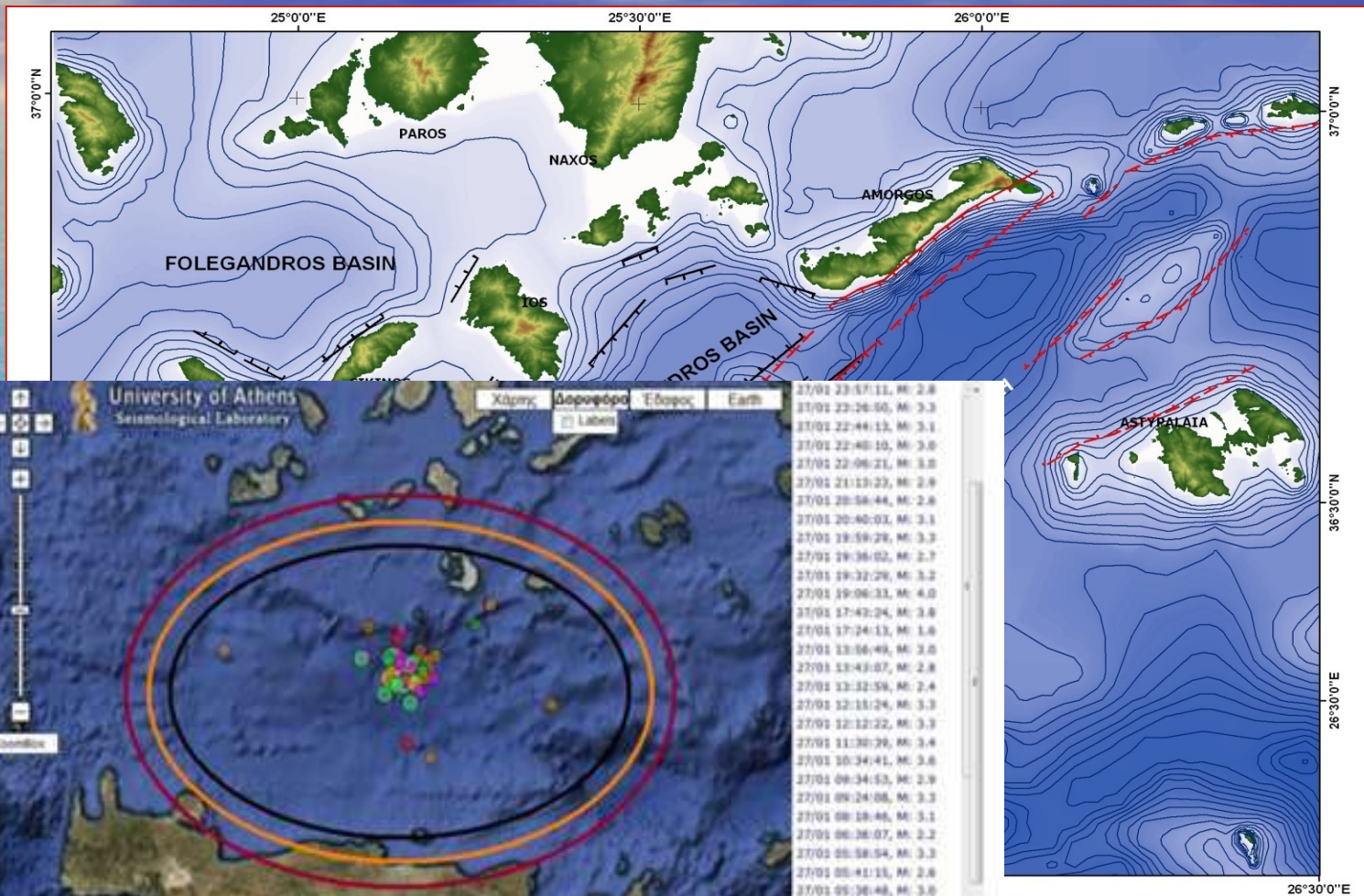
Δημητριάδης Ιορδάνης (Dimitriadis),
PhD 2008

NE- SW striking faults primarily and WNW - ESE striking faults secondarily host most of seismic activity in the south-central Aegean.

Detailed observations of surface fault kinematics and earthquake focal mechanisms can help to determine more accurately the underlying brittle tectonics and the associated stresses below



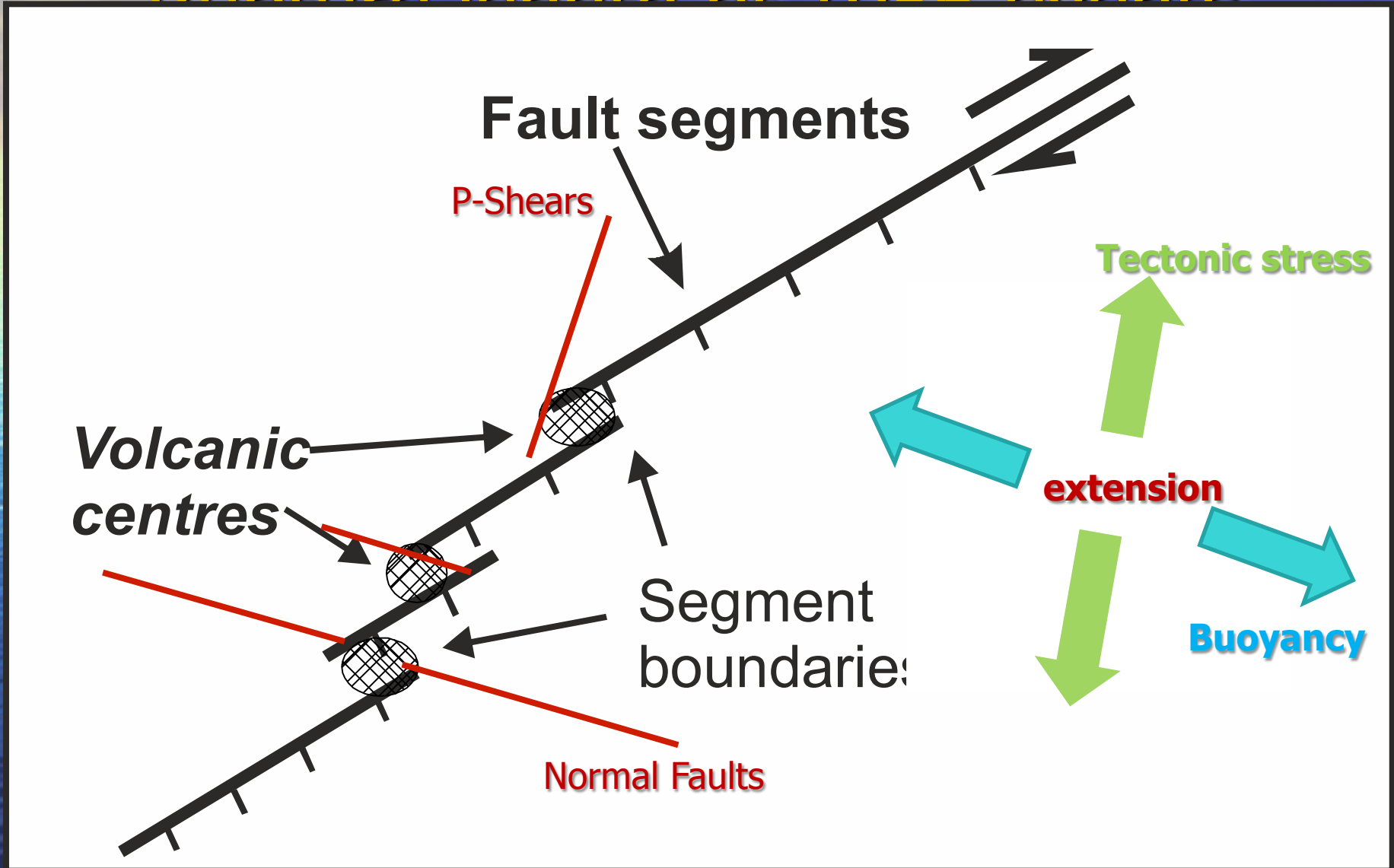
The first is a pure **extension (PE)** activating E-W to ESE-WSW trending faults as normal, NE-SW to ENE-WSW trending faults as right-lateral oblique extensional faults to right-lateral oblique-normal faults and NNE-SSE to NE-SW trending faults as right-lateral oblique extensional to strike-slip faults.



area are important in
gamma.

N

Rupture length of 1056 events



CONCLUSIONS

This work is a quantitative study of the fault geometry and kinematics of Santorini Island and surrounding area

The refined stress regimes that have been resolved through the Win-Tensor software (Delvaux, 2011) are both extensional with the first having σ_1 : 202°-85°, σ_2 : 293°-00°, σ_3 : 023°-05° and stress ratio $R= 0.42$ and the second σ_1 : 271°-83°, σ_2 : 031°-03°, σ_3 : 121°-06° and stress ratio $R= 0.2$.

The first is a pure extension (PE) activating E-W to ESE-WSW trending faults as normal, NE-SW to ENE-WSW trending faults as right-lateral oblique extensional faults to right-lateral oblique-normal faults and NNE-SSE to NE-SW trending faults as right-lateral oblique extensional to strike-slip faults. The second stress regime is a Radial-Pure Extension (RE-PE) that mainly activates N-S to NE-SW trending faults as normal ones

The volcanic centers and dykes, i.e., the magmatic feeders trend along the NNE-SSW to NE-SW tectonic lines and not along the large E-W trending normal faults

The almost vertical right-lateral oblique-extensional to strike-slip faults that act as bridges among the E-W normal faults facilitate the pull-apart geometry and basin formation, and thus the extrusion of the volcanic rocks.

conclusion

- **The fact that these stress regimes are contemporary in the area implies that the first is attributed to the tectonic stresses related with the well-established Aegean motion towards SSW, whereas the second, which gives rise to recent microseismicity of the area, is a local stress regime attributed to buoyancy forces relating the magmatic processes of the area.**
- **Therefore, the combination of these two stress regimes reflects the competition between the tectonic (lithospheric) and magmatic-(local volcanotectonic) forces, in a fault-dynamic regime that could be characterized as extensional-transtensional field.**

An aerial satellite-style photograph of the Mediterranean Sea region, showing the coastlines of Europe, Africa, and Asia. The sea is a deep blue, and the surrounding land is a mix of green and brown. The text "Thanks for your attention" is overlaid in yellow. Two small inset images are placed over the sea: one on the left and one on the right, both showing ancient-style ships and structures.

Thanks
for your attention



Ευχαριστώ
για την προσοχή σας

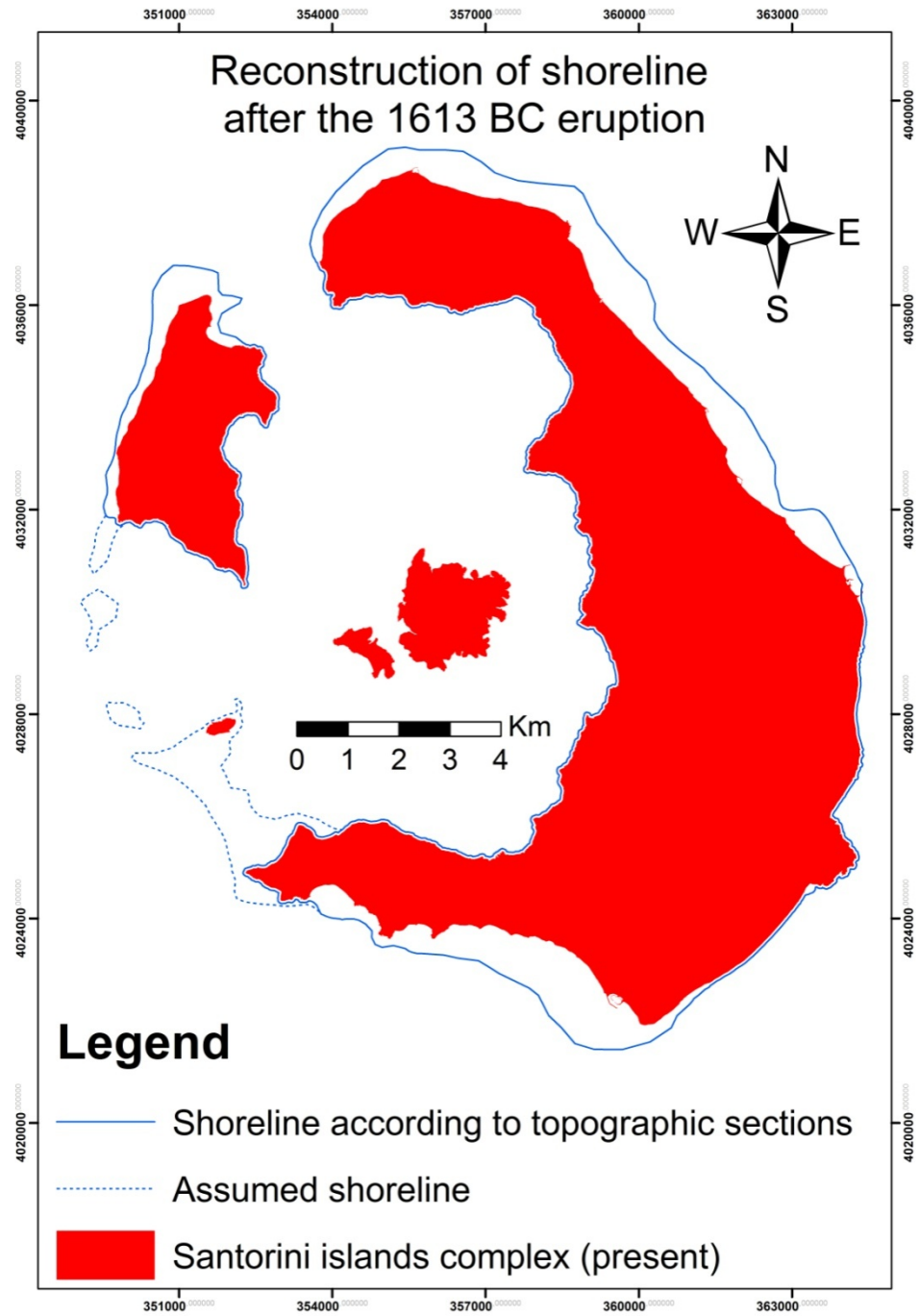
Thanks

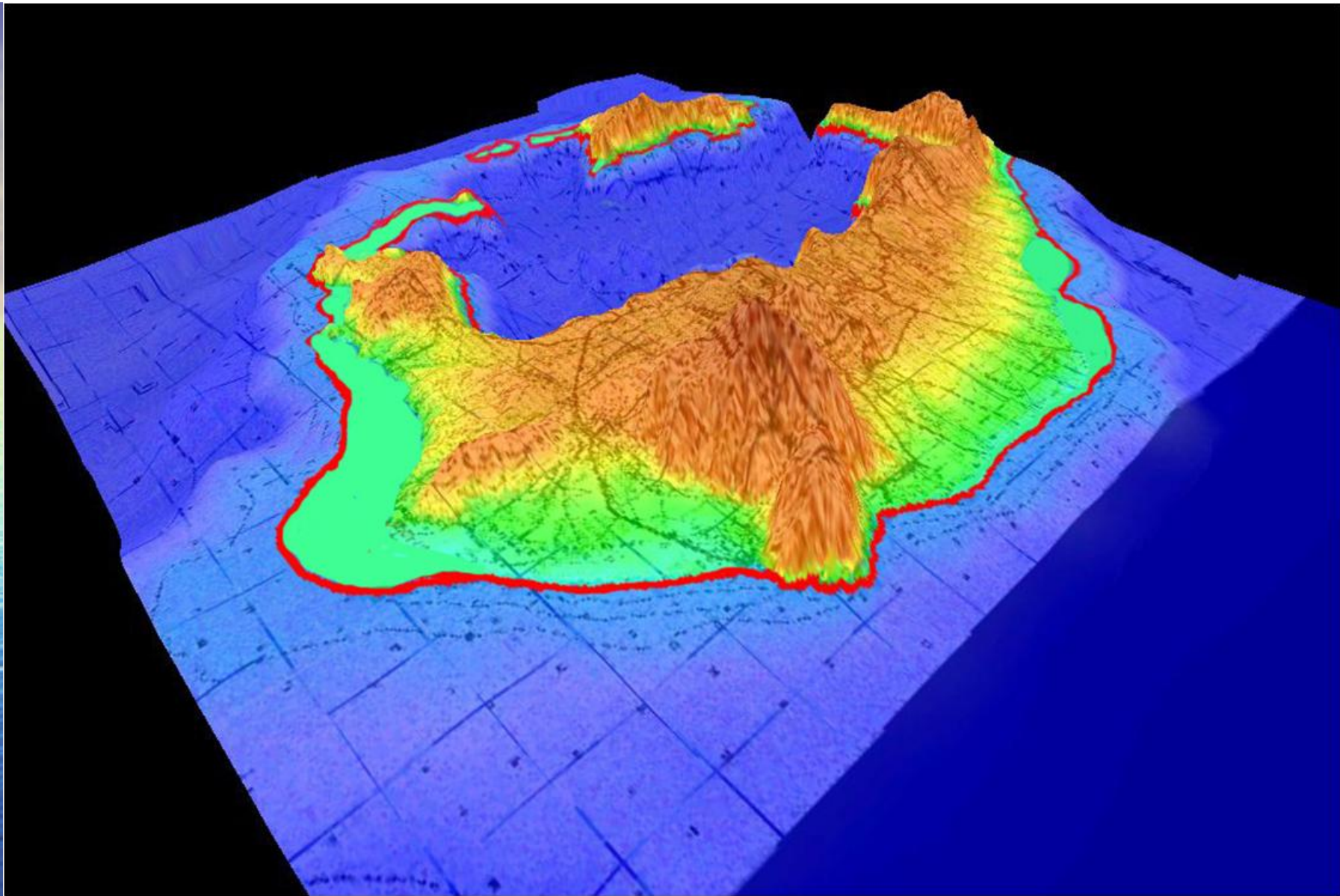
**Ευχαριστώ
για την προσοχή σας**





Reconstruction of shoreline after the 1613 BC eruption





A three dimensional view of Santorini Island, just after Minoan eruption from southeast to northwest direction

● References



- Byerlee, J.D., 1978. Friction of rocks. *Pure and Applied Geophysics* 116, 615–626.
- Delvaux. D., 2011. Win-Tensor 3.0.0 program.
- <http://users.skynet.be/damien.delvaux/tensor/tensor-index.html>.
- Tranos, M.D. 2012. Slip preference on pre-existing faults: a guide tool for the separation of heterogeneous fault-slip data in extensional stress regimes. *Tectonophysics*, 544-545, 60–74, doi: 10.1016/j.tecto.2012.03.032.

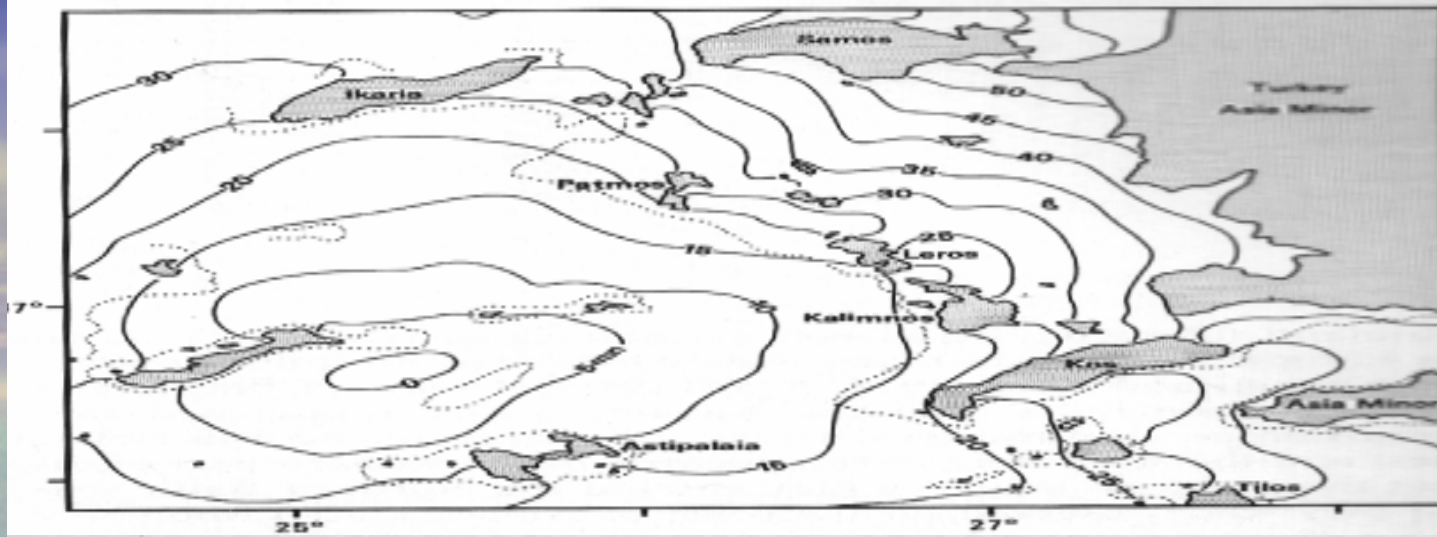
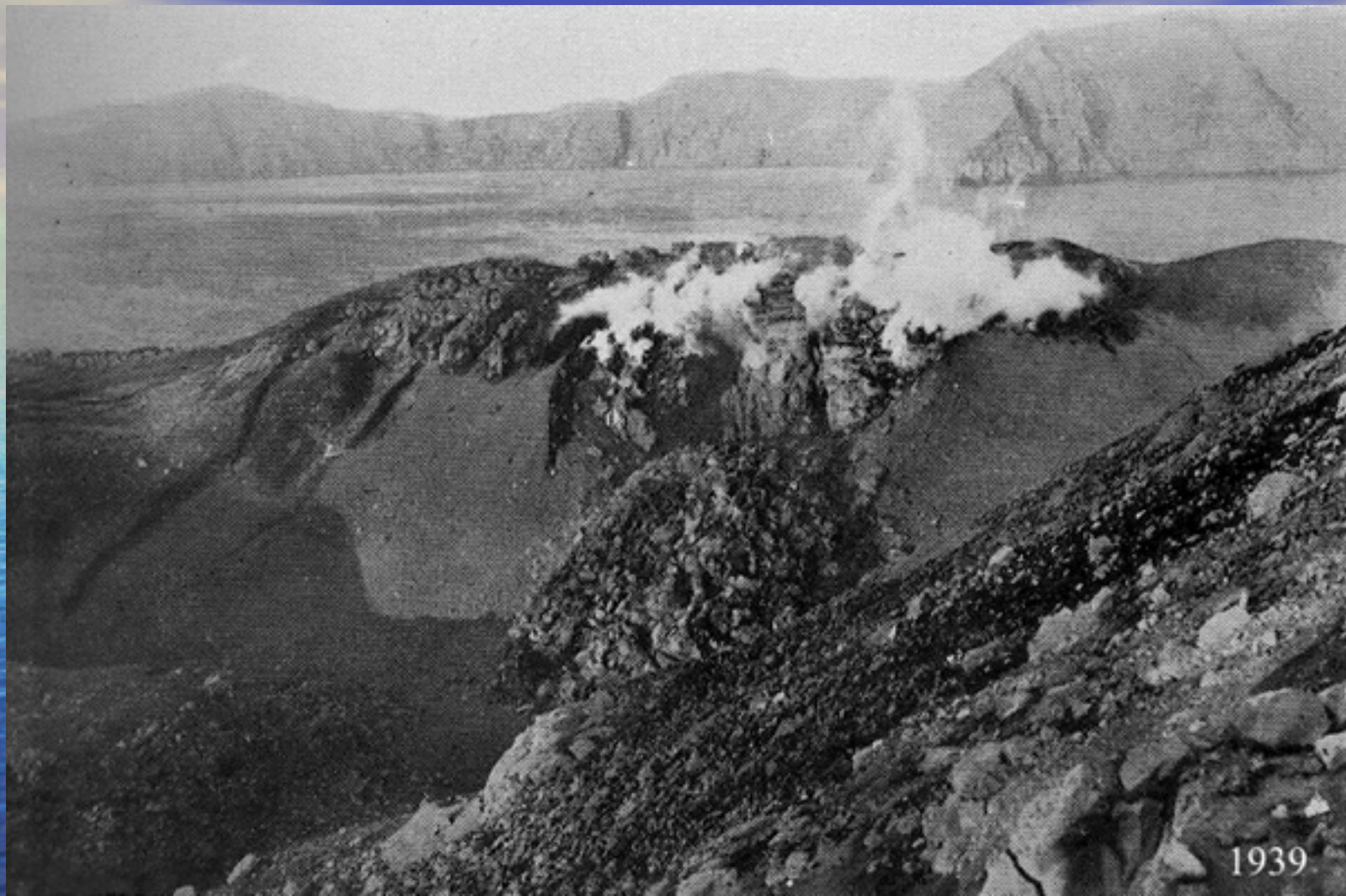


Fig. 39—Above, normal sealevel, and below, withdrawal of the waters at Skala, Patmos.



1939

The large E-W trending normal faults

The volcanic activity and more precisely the buoyancy forces could not overcome the gravity forces due to the overburden material of the hanging wall and the listric geometry of these E-W normal faults.

On the other hand the NNE- and NE-trending strike-slip faults in the Santorini area are important in localizing volcanism, providing ready pathways to deeper magma.



TR FAULT FINDER version 1.0

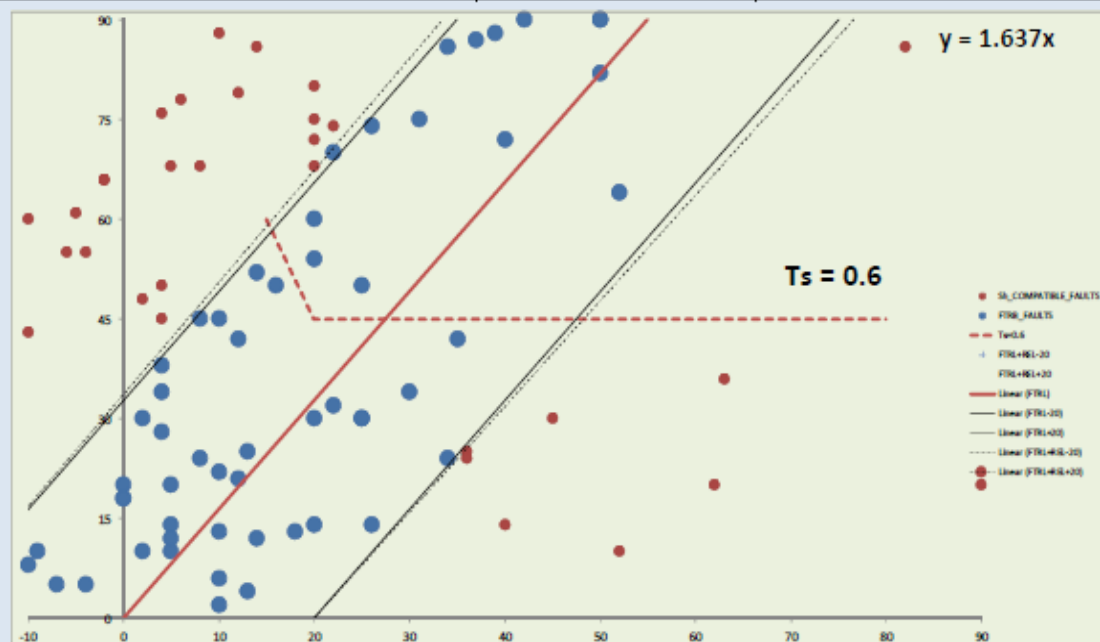
M.D.TRANOS - 2012 - ARISTOTLE UNIVERSITY OF THESSALONIKI - HELLAS

(least principal horizontal stress axis) σ_h =

120

TRL = 1.5358

FTRL = 1.6370



$R^2 =$

0.8046

NUMBER OF FAULT-SLIP DATA IN FTRB =

55

FAULTS WITH $T_s < 0.6$ =

15